NIH-PA Author Manuscript

INHIBITION OF HUMAN ACETYL- AND BUTYRYLCHOLINESTERASE BY NOVEL CARBAMATES OF (−)- AND (+)-TETRAHYDROFUROBENZOFURAN AND METHANOBENZODIOXEPINE

Weiming Luo[1,#], **Qian-sheng Yu**[1,#], **Santosh S. Kulkarni**[2], **Damon A. Parrish**[3], **Harold W. Holloway**[1], **David Tweedie**[1], **Avigdor Shafferman**[4], **Debomoy K. Lahiri**[5], **Arnold Brossi**[6], and **Nigel H. Greig**[1,*]

1*Drug Design & Development Section, Laboratory of Neurosciences, Gerontology Research Center, National Institute on Aging, National Institutes of Health, 5600 Nathan Shock Dr., Baltimore, Maryland 21224, USA.*

2*Medicinal Chemistry Section, Intramural Research Program, National Institute on Drug Abuse, National Institutes of Health, 5500 Nathan shock Dr., Baltimore, MD 21224, USA.*

3*Laboratory for the Structure of Matter, Department of the Navy, Naval Research Laboratory, Washington, D.C. 20375, USA.*

4*Department of Biochemistry and Molecular Genetics, Israel Institute for Biological Research, Ness-Ziona, 74100 Israel.*

5*Psychiatric Institute, Indiana University School of Medicine, Indianapolis, IN 46202, USA*

6*School of Pharmacy, University of North Carolina at Chapel Hill, North Carolina 27599, USA*

Abstract

A new enantiomeric synthesis utilizing classical resolution provided two novel series of optically active inhibitors of cholinesterase: (−)- and (+)- O-carbamoyl phenols of tetrahydrofurobenzofuran and methanobenzodioxepine. An additional two series of (−)- and (+)-O-carbamoyl phenols of pyrroloindole and furoindole were obtained by known procedures, and their anticholinesterase actions were similarly quantified against freshly prepared human acetyl- (AChE) and butyrylcholinesterase (BChE). Both enantiomeric forms of each series demonstrated potent cholinesterase inhibitory activity (with IC_{50} values as low as 10 nM for AChE and 3 nM for BChE), with the exception of the (+)-O-carbamoyl phenols of pyrroloindole that lacked activity (IC_{50} values > 1 μM). Based on the biological data of these four series, a SAR analysis was provided by molecular volume calculations. In addition, a probable transition state model was established according to the known X-ray structure of a transition state complex of *Torpedo californica* AChE-m-(N,N,N,trimethylammonio)-2,2,2-trifluoroacetophenone (*Tc*AChE-TMTFA). This model proved valuable in explaining the enantio-selectivity and enzyme subtype selectivity of each series. These carbamates are more or similarly potent to anticholinesterases in current clinical use; providing not only inhibitors of potential clinical relevance but also pharmacological tools to define drug-enzyme binding interactions within an enzyme crucial in the maintenance of cognition and numerous systemic physiological functions in health, aging and disease.

*To whom correspondence should be addressed: Phone: 410-558-8278; Fax: 410-558-8323, E-Mail: Greign@grc.nia.nih.gov.
#Weiming Luo and Qian-sheng Yu made equal contributions to this research and are equal first authors.

INTRODUCTION

Dementia of the Alzheimer's type afflicts some 4.5 million Americans and some 18 million people worldwide. Based on the 'cholinergic hypothesis' of memory, the depletion of its neurotransmitter, acetylcholine (ACh), and loss of associated synapses during the progression of Alzheimer's disease (AD),[1,2] cholinesterase inhibitors (ChEIs) have been synthesized and developed to clinical practice to ameliorate the associated cognitive symptoms.[3] This is achieved by reducing the rate of hydrolysis of ACh in brain and thereby augmenting its cholinergic activity. Although ChEIs and the recently FDA approved drug, memantine, are the only ones to have consistently induced improvements in cognitive function in mild to moderate AD,[4] such improvements are, unfortunately, generally modest. Indeed, recent clinical trials have triggered debate as to the relevance of the benefit of this drug class.[5,6] Such concern has prompted two avenues of research. One to develop a new generation of ChEIs with activity beyond the modest symptomatic one associated with initial agents, and another to optimize current agents based on a greater understanding of enzyme/inhibitor interactions. Our research focus has been to undertake both, simultaneously.

A classical ChEI, used to elucidate the original nature of chemical transmission of nerve action and the cholinergic system (Sir Henry Dale and Professor Otto Loewi, Nobel Prize 1936), is the natural product, (−)-physostigmine (**15a**). An alkaloid isolated from the seeds of the Calabar bean, *Physostigma venenosum*,[7–9] (−)-physostigmine (**15a**) has provided a template in the development of several AD drugs, including rivastigmine (Novartis, Basel, Switzerland), phenserine (National Institute on Aging, Baltimore, MD, and Axonyx, New York, NY), eptylstigmine (Mediolanum, Milan, Italy) and the parent compound, itself, in a slow-release formulation (*Synapton*, Forrest laboratories, St Louis, MO).[3,10,11] Extensive structure-activity relationships of this class of ChEIs indicates that (i) all derivatives of physostigmine with anticholinesterase activity are levorotary, with a 3a-*S* configuration in their pyrroloindole tricyclic ring system, and, (ii) selectivity between the two cholinesterase forms, acetyl- (AChE: EC3.1.1.7) and butyrylcholinesterase (BChE: EC 3.1.1.8), is primarily correlated with the structure of the N-substituted moiety of the carbamoyl side chain.[10–12]

An exception to the enantiomeric selectivity of physostigmine derivatives is the N^1-nor series of derivatives.[13,14] (−)-Physovenine (**20a**), a congeneric alkaloid of physostigmine,[9,10] also lacks enantiomeric selectivity.[10,15,16] The (+)-isomers of these two series of compounds, interestingly, have unexplainable anticholinesterase activity.[13–16] In our continuing effort to design new and improved ChEIs, we recently successfully synthesized two novel series of bio-active racemic carbamates with the tricyclic skeletons, furobenzofuran and methanobenzodioxepine.[17] Herein, we describe the synthesis and activity of their optically pure enantiomers with the dual purpose of (i) developing new AD drug candidates and (ii) utilizing them as tools to elucidate the molecular interactions required by the tricyclic skeleton of this important class of ChEI to achieve enantio-selectivity within AChE and BChE.

RESULTS

Chemistry

The starting material, 5-hydroxy-3-methyl-3-methoxycarbonylmethylene-benzofuran-2-one (**1**), was produced from C3-alkylation of the condensation product of 1,4-cyclohexandione and pyruvic acid, according to a previously reported procedure.[17] First, compound **1** was reacted with (−)-menthyl chloroformate to provide a mixture of the stereoisomers of (3*S*) and (3*R*)-menthylcarbonates of 5-hydroxy-3-methyl-3-methylacetate-benzofuran-2-one **2** and **3** (Scheme 1).

Since it proved difficult to isolate stereoisomer **2** and **3** with chromatography, we separated them by repeated crystallization. This was performed from hexane, at first, and then from ethanol to eventually yield two separate crystals with different crystalline forms: needle (**2**) and flaky (**3**) (Experimental Section).

The absolute configuration of the C-3 position was determined based on the known configurations of C-19, C-21 and C-24 from compound **3** by X-ray crystallography. Figure 1 shows that compound **3** has a *R* configuration at its 3-position. As a consequence, compound **2** should possess a *S* configuration at its 3-position. The use of chiral HPLC to measure the optical purity of compounds **2** and **3** proved unsuccessful. The hydrolysis of stereoisomer **2** and **3** provided (−)-enantiomer **4**, $[\alpha]_D^{26}$ −2.6° (C=0.62, CHCl$_3$), and (+)-enantiomer **5**, $[\alpha]_D^{27}$ +2.2° (C=0.45, CHCl$_3$) (Scheme 1), respectively. The enantiomeric excesses value (ee %) of each was measured by chiral HPLC analysis and reported in the Experimental Section (Figure 2). Compounds **4** and **5** were, for practical purposes, optically pure. In the process of reduction, the stereochemistry at the 3-position of compounds **2** and **3** was unchanged. Hence, **2** gave **6a** (3a*S*-configuration) and **7a** (5*S*-configuration); whereas, **3** gave **6b** (3a*R*-configuration) and **7b** (5*R*-configuration). The probable mechanism underpinning this reductive cyclization has recently been published.[17, 18] In our recent prior research, we reported that the reductive cyclization of (±)-5-hydroxy-3-methyl-3-methylaceta-tebenzofuran-2-one by LiAlH$_4$ gave tetrahydrofurobenzofuran and methanobenzodioxipene in a yield of 10%.[17] In the present report, the reductive lithium-aluminum complexes of compound **2** and **3** were acidified by 1M HCl in anhydrous Et$_2$O, instead of oxalic acid, to elevate the yield to approximately 30% (Scheme 2).

Phenols **6a** and **7a**, as well as **6b** and **7b** were reacted with different isocyanates to give 6 pairs of corresponding carbamates: **8a** and **11a**, **9a** and **12a**, **10a** and **13a**, as well as **8b** and **11b**, **9b** and **12b**, **10b** and **13b**, respectively. Thereafter, each of these pairs of compounds was separated by preparative TLC, utilizing a procedure reported previously.[17]

The syntheses of carbamates of the physostigmine and physovenine series of analogues are shown in Scheme 3. Compounds **15a** and **b**, **17a**, **18a**, **20a** and **b**, **22a** and **23a** are known compounds.[15,16] Compounds **16a** and **21a** were synthesized from compounds **14a** and **19a**, which were obtained from natural physostigmine according to a known procedure.[17] Compounds **17b**, **18b**, **22b** and **23b** were synthesized from (+)-3a(*R*)-eseroline (**14b**) and (+)-3a(*R*)-physovenol (**19b**). These phenols, (**14b**) and (**19b**), were obtained by asymmetric syntheses starting from N-methylphenetidine.[14]

X-ray Crystallography

The results of the X-ray studies of compound **3** are illustrated in Figure 1. The chirality of the asymmetric center are as follows: C3-*R*, C19-*R*, C21-*R* and C24-*S*. The six-membered ring of the menthyl moiety has a chair conformation; in contrast, the benzofuran system is flat.

Biological Evaluation

Table 1 shows the anticholinesterase activity of enantiomers **8–13**, **15–18** and **20–23** against freshly prepared human AChE and BChE, derived from erythrocytes and plasma, respectively. The concentration of compound required to inhibit 50% enzyme activity (IC$_{50}$ value) was quantified by a modified Ellman technique,[13–17, 19–21] and values for *R*-configuration versus *S*-configuration are represented by the symbol *R/S*. A smaller IC$_{50}$ is associated with a lower *K*i value and a higher affinity of inhibitor-enzyme binding.[22–24] A *R/S* value of 1 is indicative of similar inhibitory activity for the *R*- and *S*-configurations. For a *R/S* value >1, the compound with a *R*-configuration has a lower potency than its enantiomer.

With the sole exception of the compound pair, **17a** and **17b**, that possessed low and approximately similar BChE inhibitory activity (*R/S*=0.6), all compounds with a *S*-configuration proved to be more potent than their corresponding enantiomer (*R/S* > 1). This was most evident in the physostigmine series, where AChE inhibitory activity was achieved with a *R/S* value ≥ 353 and BChE inhibitory action was achieved with a *R/S* value ≥ 102. Hence, in the physostigmine series, carbamates of (+)-physostigmine (**15b**, **17b**, **18b**) possess minimal cholinergic activity, quite the opposite of their potent (−)-enantiomers.

In complete contrast with the physostigmine series, both enantiomers of the novel tetrahydrofurobenzofuran (**8a** and **b**, **9a** and **b**, **10a** and **b**) and dihydrobenzodioxepine (**11a** and **b**, **12a** and **b**, **13a** and **b**) series possessed potent anticholinesterase action for AChE, BChE or both, with *R/S* values of ≤9.3. This activity is in accord with the congener, physosvenine carbamates (**20a** and **b**, **21a** and **b**, **22a** and **b**, **23a** and **b**) that are similarly active in both enantiomeric forms with a preference for the *S*-configuration. As described, N-demethylation of physostigmine (**15a**) minimizes the enantio-selectivity of this series,[14] which suggests that the N^1-substitution of the tricyclic ring is a key determinant regarding enantio-selectivity. Additionally, the development of members of the tetrahydrofurobenzofuran and dihydrobenzodioxepine series to clinical development could be undertaken with either the potent *S*- (−)-enantiomers or the racemates, whose synthesis would be far easier and cheaper (avoiding optical resolution) and whose anticholinesterase activity is almost equal. A comparison of Table 1 and Table 2, the latter defining the anticholinesterase activity of agents of current and recent clinical interest against enzyme drawn from the same individual and analyzed similarly, suggests that compounds **9a**, **12a** and **10a**, **13a** possess sufficient potency and selectivity for AChE and BChE, respectively, to be of clinical interest.

In each of the four series of compounds detailed in Table 1, the differential selectivity for AChE or BChE is determined by the structure of N-substituted moiety of the carbamate. Specifically, the N-methyl carbamates provide minimal enzyme subtype selectivity. The N-ethyl carbamates have a moderate BChE preference. The N-2'-methylphenylcarbamates have high AChE selectivity and N-4'-isopropylphenylcarbamates reverse this and demonstrate a high BChE preference. Of particular note, the AChE and BChE selectivities of the novel tetrahydrofurobenzofuran and dihydrobenzodioxepine series are amongst the greatest found of all ChEIs yet synthesized on the tricyclic backbone of physostigmine.

DISCUSSION

Molecular comparison by volume calculations

As all of the described carbamates possess close structural similarity as well as a similar inhibitory mechanism, we can initially compare them by means of superimposition to further elucidate the basis of their enantio-selectivity. This was undertaken for the four AChE potent inhibitors with *S*-configuration carbamates (**9a**, **12a**, **17a** and **22a**) by generating a 'molecular volume map' of each molecule that corresponds to their van der Waals surface.[25,26]

As illustrated in Figure 3, for each compound, the relative positions of their two phenyl moieties, on either side of the carbonyl group in their optimized conformation, were almost identical – closely overlaying one another. These four compounds could be closely superimposed, except for disparity in their tricyclic systems. The combined molecular volume map of compounds **9a**, **12a**, **17a** and **22a** provides an 'enzyme – excluded map' (green area in Figure 3), within which all active compounds should fit. The molecular volume of the *R*-2'-methylphenyl carbamates, **9b**, **12b**, **17b** and **22b**, minus the enzyme – excluded volume provides an 'estimate volume' that represents the additional volume generated by that of each *R*-isomer (yellow meshed area within Figure 3).

As shown in Table 3, the lowest estimate extra volume of compound **9b** (7.1 Å^3) corresponds to the lowest enantio-selectivity (R/S = 1.8). The highest estimate extra volume (24.8 Å^3) of compound **17b** corresponds to the highest enantio-selectivity (R/S = 551). Specifically, the larger estimate extra volume of compound **17b** (yellow meshed area in Figure 3) likely seriously hinders the approach to and hence binding between the inhibitor and enzyme. Molecular modeling studies were undertaken to aid elucidate how this additional estimate extra volume hinders binding.

Molecular model of the transition state

The wide structural diversity of available ChEIs suggests that unlike types of inhibitors bind with AChE in different ways via disparate yet specific interactions between compound and enzyme.[27–29] Most anticholinesterases, such as those in Table 2 as well as the potent non-clinical tacrine-based triazoles and other hybrids, are cationic at physiological pH; whereas some, including those of the present study and arisugacin, are not.[30–32] Human cholinesterases are large complex molecules composed of catalytic subunits that can clearly accommodate a variety of specific binding interactions associated with these diverse inhibitors. They contain up to 583 amino acids, a Mr of 70–80 kDa, and are variably glycosylated.[29,33]

Three-dimensional analyses of AChE and BChE, based on x-ray crystallography, have provided structural information regarding the positioning of the catalytically important amino acid residues within these proteins.[34–41] In synopsis, three major binding domains have been described within AChE and two within BChE in an internalized, primarily hydrophobic gorge of some 20 Å length, but as narrow as 0.5 Å wide. Deepest within this gorge is a catalytic 'acyl' binding domain, which hydrolyses choline esters through electron transfer within a catalytic triad, termed a 'charge relay system. The triad includes a Ser_{200}, the imidazole group of a His_{440}, and the carboxylic acid moiety of a Glu_{327} (*Tc*AChE numbering). A 'choline' binding domain resides midway along the gorge, and a 'peripheral' anionic site exists at the gorge mouth for AChE but not BChE,[30–41] and this latter site may be involved in the complexing of AChE with amyloid-β peptide in the Alzheimer brain.[42] Notably, the neurotoxicity associated with Aβ-AChE complexes has been shown to be greater than that induced by the Aβ peptide alone in both cell culture and animal experiments.[39]

On the basis of calculations and electro-optical measurements, it has been suggested that electrostatic charges associated with seven negatively charged amino acids residues close to the entrance of the gorge trap and steer charged ligands into its mouth.[43,44] In the case of ACh, the quaternary choline moiety interacts with Trp_{84} of *Tc*AChE and, to a lesser extent, with Phe_{330} within the choline binding domain. This orientates the compound to allow the approach and nucleophilic attack of the catalytic triad on its carbonyl group. A quaternary transition state between Ser_{200} and ACh momentarily exists that then rapidly collapses into an acylated-enzyme intermediate and released choline. Thereafter, prompt hydrolysis of the acetylester reactivates the enzyme to allow efficient cleavage of as many as 10^4 ACh molecules per second.[37,38] (−)-Physostigmine (**15a**) and analogues interact similarly with the same two binding domains. However, nucleophilic attack of its carbonyl moiety results in a transient (−)-physostigmine-AChE intermediate, in a tetrahedral conformation, that then swiftly collapses to a carbamylated drug-enzyme complex that is dramatically more stable than the acetyl enzyme one associated with ACh; enzyme inhibition occurs consequent to the slow rate of enzyme decarbamylation. The inhibition process, hence, involves AChE-catalyzed hydrolyses of inhibitors.[37,38] In such a chemical reaction, the highest energy transition state controls the overall rate of the reaction. A catalytic enzyme can lower this energy barrier by specific interaction with the inhibitor in the transition state (**24 – 25**).[45] (Scheme 4). As shown in Table 1, each of the eight different carbamates with a same N-substituted side chain (e.g., **8 a** and **b**, **11 a** and **b**, **16 a** and **b**, **21 a** and **b**) should generate identical carbamylated enzyme structures

after their reaction with either AChE or BChE. Hence their different IC_{50} values should be related to their affinities and rates of carbamylation, and not to decarbamylation – which would impact the time-dependence of the inhibition associated with each. As a consequence we can focus on carbamylation due to the short time frame of our biological studies.

A better insight into the molecular interactions of the enzyme and inhibitor can be obtained at the transition state. Whereas it is not currently possible to produce a crystal structure of an enzyme complexed with its substrate in the transition state, due to the short transition state lifetime versus the time required for X-ray data collection, one can exploit the high affinity of transition state analogues. In this regard, the analogue, m-(*N,N,N*-trimethylammonio)-2,2,2-trifluoroacetophenone (TMTFA), possessing a low Ki (15 fM) for inhibition of TcAChE,[46] was utilized to aid model the interaction of our compounds within the active site of AChE.

Prior investigation of the X-ray crystallographic structure of *Tc*AChE complexed with the known physostigmine analogue, MF268 (8-(cis-2,6-dimethylmorpholino) octylcarbamoyleseroline), demonstrated the presence of a covalent bond between the carbonyl carbon and γ-O of Ser_{200}, and that the N-substituted side chain of the carbamoyl moiety is located inside the acyl-binding pocket and extends to the rim of the active site gorge.[47,48] The X-ray crystallographic transition state analogue structure of *Tc*AChE-TMTFA (code 1AMN) was obtained from the RCSB protein databank. After extraction of TMTFA, the (−)-(3a*S*)-N-2'-methylphenylcarbamoyl phenol of furobenzofuran (**9a**) was docked, in accord with knowledge gained from the binding of MF268.[47,48]

As shown in Figure 4, six hydrogen bonds are apparent within the model (yellow lines): the NH of Gly_{118}, Gly_{119} and Ala_{201} with the oxygen of the ligand carbonyl, the γ-O of Ser_{200} with a single H, the hydrogen with N of His_{440}, and the NH of His_{440} with the oxygen of Glu_{327}. Together with the covalent bond of the γ-O of Ser_{200} with the C of the ligand's carbonyl group, the illustrated hydrogen bonds comprise an acylation site. This site is considered as a crucial part of the transition state. A transition state model was developed by (i) keeping the acylation site intact (by constraining the relative distances between the described atoms) and, (ii), minimizing the complex energy, after automatic adjustment of the conformation of the remaining complex.

This model resembles a 'beam balance'. The central supporting point is a covalent bond between the γ-O of Ser_{200} and the C of the ligand's carbonyl group. The π-π interaction system between the N-phenyl group of carbamate (**9a**) and the phenyl group of Phe_{288} of the enzyme comprises one side of this balance. The π-π or lipophilic (C–H¨π) interaction system of the furobenzofuran moiety of compound **9a** and the indole system of Trp_{84} of the enzyme forms the other side of the balance. Such C–H¨π interactions have been observed in the x-ray crystal structure of other neutral molecules with *Tc*AChE.[49] Any change on either side of this balance may adversely affect the formation of the transition state. Utilizing this model, we can revisit the basis of enantio-selectivity and enzyme subtype selectivity.

Enantio-selectivity

As shown by molecular volume calculations (Figure 3, Table 3), for all carbamates with a *R*-configuration, with the exception of the physostigmine series, their molecular volumes are not greatly different. This would support the lipophilic interaction between the tricyclic ring system of the ligands and the indole system of Trp_{84} of the enzyme. Hence, all of these compounds retain substantial anticholinesterase activity compared to their *S*-isomers.

The only exception involves *R*-configuration compounds having a N^1-methyl group (the physostigmine series). The model predicts that the N^1-methyl group will become inserted between the tricyclic ring system and the indole system of Trp_{84}. The lipophilic interaction

will consequently disappear, and a transition state between ligand and enzyme complex would not be readily formed without this lipophilic interaction. As a result, the (+)-physostigmine analogues **15b**, **17b** and **18b** would be predicted to possess a poor AChE and BChE inhibitory action, in accord with their measured poor ChEI activity.

Enzyme subtype selectivity

The acyl-binding pockets within AChE and BChE differ from one another in size and shape. The pockets can be differentiated on the basis of two amino acid residues located at the bottom of the acyl-loop. These residues are aromatic in AChE (Phe_{288} and Phe_{290}) but aliphatic in BChE (Leu_{286} and Val_{288}).[33,35,37,38,46] The latter pocket, hence, is slightly larger due to the smaller protruding side chains associated with Leu and Val.[12].

Our previous studies have shown that the conformational energy barrier of the N-phenyl group of compound **17a** and its analogues, rotated around C1'-N bond, is correlated to the IC_{50} of AChE. A higher energy barrier is associated with a lower inhibitory activity (a larger IC_{50}); although, inexplicably, the energy barrier is as low as 0–0.7 kcal/mol. [21]

According to the described transition state model (Figure 4), the π-π interaction system between the N-phenyl group of the carbamate (**17a**) and the phenyl group of Phe_{288} of the enzyme comprises one side of this balance. Rotation of the N-phenyl group will decrease this π-π interaction and directly influence the stability of the transition state; consequently lowering the affinity between ligand and enzyme. [21]

Utilizing the same model, we can now propose a basis for the cholinesterase subtype selectivity of the different carbamates moieties. (i) The small methyl group of N-methylcarbamates has almost no lipophilic interaction with residues of the acyl pocket, it thus has little influence on this balance and hence there is minimal subtype selectivity between AChE and BChE for N-methyl carbamates of all series. (ii) The ethyl group of N-ethylcarbamates, likewise, has relatively meager, but, nevertheless, greater lipophilic interaction than N-methylcarbamates. The direction of this interaction is more favorable to form a stable transition state within BChE than AChE. Hence, all of N-ethyl carbamates possess a moderate BChE selectivity. (iii) The phenyl group of N-phenylcarbamates provides a significant lipophilic interaction with the aromatic ring of Phe_{288}. This interaction together with the lipophilic interaction between the tricyclic ring system and indol moiety of Trp_{84} provides a highly stable transition state. Thus, all N-phenyl and N-methylphenyl carbamates possess potent AChE activity. Within BChE, however, Phe_{288} is replaced by an amino acid with an aliphatic residue. A similar π-π interaction cannot be formed and leads to an unfavorable stability in the transition state, and consequent weak BChE inhibitory activity. N-phenyl and N-methylphenyl carbamates hence have high AChE selectivity. Finally, (iv) the 4'-isopropylphenyl moiety of N-4'-isopropylphenyl carbamates cannot achieve a π-π interaction within the acyl-binding pocket of AChE consequent to the bulk and hindering action of the isopropyl moiety. Within BChE, however, the lipophilic interaction of the isopropylphenyl group with residues of BChE in its larger acyl-binding pocket is favored (consequent to replacement of AChE Phe_{288} and Phe_{290} by Val and Leu), which stabilizes the transition state. Thus all of the N-4'-isopropylphenyl carbamate series have a potent and selective BChE inhibitory action.

In accord with this, one of the most potent and selective BChE inhibitors in the physostigmine series, (−)-N^1-phenethylnorcymserine (**26**) (IC_{50}: AChE >30,000 nM, BChE 6.0±1.0 nM, selectivity >5000-fold BChE) (Fig. 5),[19] similarly can fit within the elongated acyl binding pocket associated with BChE. However, as the N^1-phenethyl moiety is directed outside the lipophilic interaction system, activity is not perturbed. Indeed, it is augmented, likely, as a consequence of hydrophobic interactions close to the gorge mouth. Interestingly, the elongated (−)-4'-benzoxyphenyl carbamate of physostigmine, **27** (Fig. 5),[50] that lacks a hindered 4'-

isopropyl group, can maintain the π-π interaction associated with potent AChE binding, but make use of the larger acyl pocket associated with BChE to achieve BChE inhibitory potency (IC_{50}: AChE 58±4 nM, BChE 7.0±1.0 nM, selectivity 7-fold BChE). [50]

In synopsis, we report a new enantiomeric synthesis, through classical resolution, of two novel series of potent anticholinesterases: the O-carbamoyl phenols of furobenzofuran and benzodioxepine. These two series provide candidates to selectively inhibit either AChE or BChE and, additionally, include some that possess neurotrophic actions.[17] Such actions may or may not be cholinergically mediated and provide this class of drugs actions beyond those that are classically considered to be only symptomatic.[51,52] Carbamates of these novel series are sufficiently active to be of potential clinical interest, comparing favorably with the inhibitory action of approved and recent ChEIs (Table 2, Figure 6), and could be developed either as their potent *S*-enantiomers or as their synthetically cheaper racemates. In addition, their enzyme subtype selectivity compare favorably with the classical selective anticholinesterases, BW284c51 and iso-OMPA. Based on the described molecular volume calculations and known X-ray structure of a transition state complex of *Tc*AChE-TMTFA, we have developed a beam balance-like transition state model of the *Tc*AChE-N-phenylcarbamate complex. Using this model, we can now propose a basis to account for the enantio-selectivity of physostigmine and its congeners.

Experimental Section

Chemistry

Melting points (uncorrected) were measured with a Fisher-Johns apparatus; ^{1}H NMR and ^{13}C NMR were recorded on a Bruker (Bellevica, MA) AC-300 spectrometer; MS (m/z) were recorded on a Hewlett-Packard 5973 GC-MS (CI); HRMS were performed by the UCR Mass Spectrometry Facility, Department of Chemistry, University of California; Optical rotations were measured by JASCO, Model DIP-370 (Japan, Spectroscopic Co., LTD.); Elemental analyses were performed by Atlantic Microlab, Inc.; The ee% value of optically active compounds was determined by HPLC analyses using a HP1100 instrument and a chiral column (ChiraDex® 5µm) (Agilent Technology), mobile phase MeOH/H_2O = 45/55, elution rate 0.5 ml/min., UVD 254 nm – all at room temperature. All reactions involving non-aqueous solutions were performed under an inert atmosphere.

(3*S*) And (3*R*)-Menthyl carbonates of 5-hydroxy-3-methyl-3-methylacetate-benzofuran-2-one (2) and (3)

Under a nitrogen atmosphere, a solution of 5-hydroxy-3-methyl-3-methoxycarbonylmethylenebenzofuran-2-one (**1**) (116mg, 0.491mmol) in 0.06 mL of triethylamine and 1.5mL of benzene was dropwise added into (−)-menthyl chloroformate (118mg, 0.539mmol) at room temperature. The mixture was stirred for 1.5 hours at the same temperature. The crude product was subjected to chromatography on silica gel (EtOAc/Hexane=1/3) to give 156.5 mg of white crystalline product, yield 76.2%: ^{1}H-NMR (CDCl_3) δ 7.20-7.02 (m, 3H, Ar-H), 4.68-4.52 (m, 1H, CH-OC=O), 3.53 (s, 3H, CH_3O), 3.10, 2.96 (AB, J_{gem}=17.6Hz, 2H, C3-CH_2COO), 2.21-2.11 (m, 1H, CH-^{i}Pr), 2.10-1.98 (m, 1H, CHMe), 1.80-1.65 (m, 1H, CHMe_2), 1.51 (s, 3H, C3-CH_3), 1.59-1.41 (m, 2H, CH_2COC=O), 1.26-0.80 (m, 4H, CH_2CH_2), 0.97 (d, 6H, CH_3CCH_3) and 0.85 (d, 3H, CH_3CCCOC=O) ppm; CI-MS (CH_4), m/z: 419(MH^+), 418, 417, 371, 237, 181, 153 and 109; HR-MS m/z: Calcd for $C_{23}H_{34}NO_7$(MNH_4^+): 436.2335; Found: 436.2326. The above white crystal product was, thereafter, recrystallized from both hexane and ethanol, separately, several times, until the optical rotations and melting points of the two different isolated crystalline forms did not change. One, a needle crystalline form, was product **2**: m.p. 106.8–107.4°C; $[\alpha]_D$ [25]-60.8°

(c=0.53,CHCl$_3$). Anal. (C$_{23}$H$_{30}$O$_7$) C, H. The other, a flaky crystalline form, was product **3**: m.p.148.0–148.8°C; [α]$_D^{26}$-19.7 °(c=0.74,CHCl$_3$). Anal. (C$_{23}$H$_{30}$O$_7$) C, H.

(−)-(3*S*)-5-Hydroxy-3-methyl-3-methylacetate-benzofuran-2-one (4)

Under a nitrogen atmosphere, a mixture of reactant **2** (0.493g, 1.178 mmol) and sodium hydroxide (0.2g, 5.0 mmol) in 18 mL of methanol was stirred for 1.5 hours at room temperature. It was then neutralized with 1N HCl. After removing solvent, the residue was chromatographed on silica gel (CH$_2$Cl$_2$/MeOH=10/1) to give 168.2 mg of product **4**, yield 60.4%: m.p. 157.0–159.0 °C; [α]$_D^{26}$ −2.6 °(c=0.62,CHCl$_3$); ee%=100% (HPLC); ^{1}H-NMR (CDCl$_3$) δ 6.92-6.61 (m, 3H, Ar-H), 5.07 (s, 1H, OH), 3.44 (s, 3H, OCH$_3$), 3.02, 2.84 (AB, J$_{gem}$=18.0Hz, 2H, C3-CH$_2$C=O) and 1.41(s, 3H, C3-CH$_3$) ppm; CI-MS (CH$_4$), m/z: 237(MH$^+$), 205, 177 and 163.

(+)-(3*R*)-5-Hydroxy-3-methyl-3-methylacetate-benzofuran-2-one (5)

Compound **5** was prepared as described above, yield 66.0%: m.p. 156.0–158.6 °C; [α]$_D^{27}$+2.2 °(c=0.45,CHCl$_3$); ee%=100%. The ^{1}HNMR and CI-MS (CH$_4$) are the same as that of compound **4**.

(3a*S*)-5-Hydroxy-3a-methyl-2, 3,3a, 8a-tetrahydrofuro[2,3-*b*] benzofuran (6a) *and* (5*S*)-7-Hydroxy-5-methyl-4, 5-dihydro-2, 5-methano-1, 3-benzodioxepine (7a)

Under a nitrogen atmosphere, a solution of compound **2** (177 mg, 0.423mmol) in 2mL of ether was dropwise added to lithium aluminum hydride (32 mg, 0.843 mmol) in ether at 0°C. The mixture, after stirring at 0°C for 0.5h, was stirred for another one hour at room temperature. Thereafter, 1M HCl ether solution and was to provide a mixture of pH 3–4, which then was stirred for 0.5 hour at room temperature. Next, the mixture was filtered and the filtrate was concentrated. The residue was subjected to chromatography on silica gel (EtOAc/Hexane=1/3) to give 24.4 mg of a mixture of compounds **6a** and **7a**. The GC-CI-MS and ^{1}H-NMR of this mixture were the same as that of the racemic[17] and showed an approximate 1:1 molar ratio of (3a*S*)-5-hydroxy-3a-methyl-2, 3,3a, 8a-tetrahydrofuro[2,3-*b*] benzofuran (**6a**) and (5S)-7-hydroxy-5-methyl-4, 5-dihydro-2, 5-methano-1, 3-benzodioxepine (**7a**). The yields were 30% and the compounds were directly used as starting material for the next reactions.

(3a*R*)-5-Hydroxy-3a-methyl-2, 3,3a, 8a-tetrahydrofuro[2,3-*b*] benzofuran (6b) and (5*R*)-7-Hydroxy-5-methyl-4, 5-dihydro-2, 5-methano-1, 3-benzodioxepine (7b)

Compounds **6b** and **7b** were prepared from compound **3**, according to the procedure described for compounds **6a** and **7a**.

(−)-(3a*S*)-3a-Methyl-2, 3,3a, 8a-tetrahydrofuro[2,3-*b*] benzofuran-5yl *N*-ethyl carbamate (8a) and (−)-(5*S*)-5-Methyl-4, 5-dihydro-2, 5-methano-1, 3-benzodioxepin-7yl *N*-ethyl carbamate (11a)

Under a nitrogen atmosphere, two small pieces of sodium (about 1 mg) were added into a solution of mixture of **6a** and **7a** (24.4 mg, 0.127 mmol) in 5 mL of anhydrous ether at room temperature. This mixture was then stirred for 2 minutes, and ethyl isocyanate (30.1 µL, 0.381 mmol) was next added to the reaction mixture in one portion. An hour into the reaction at room temperature, 1.4 mL of water was added and the ether layer was separated. After drying over sodium sulphate and filtering, the filtrate was evaporated to remove solvent. The residue was chromatographed on silica gel plate (EtOAc/Hexane =1/3) to afford products **8a** and **11a**. Product **8a** (11.6 mg, 69.7%): [α]$_D^{26}$ −92.2° (c=0.09, CHCl$_3$); e.e.100%; ^{1}H-NMR (CDCl$_3$) δ 6.87-6.60 (m, 3H, Ar-H), 5.77 (s, 1H, C8a-H), 4.89 (s, br, 1H, NH), 4.06-3.56 (m, 2H, C2-H), 3.23 (m, 2H, C5-CH$_2$NHCOO), 2.13-1.91 (m, 2H, C3-H), 1.47 (s, 3H, C3a-CH$_3$) and 1.14 (t, 3H, C5-CH$_3$CH$_2$NHCOO) ppm; CI-MS (CH$_4$), m/z: 264 (MH$^+$), 193, 175 and 72. Anal. (C$_{14}$H$_{17}$N O$_4$) N, H; C: Calcd. 63.87; Found 63.14. Product **11a** (14.1 mg, 84.6%): [α]$_D^{25}$

−10.0°(c=0.12, CHCl₃), e.e.100%. ¹H-NMR (CDCl₃) δ 6.82-6,67(m, 3H, Ar-H), 5.69 (d, J=1.80Hz, 1H, C2-H), 4.88 (s, br, 1H, C7-NHCOO), 4.17, 3.70 (AB, J$_{gem}$=7.20Hz, 2H, C4-H), 3.22 (m, 2H, C-7CH₂NHCOO), 2.19-1.19 (m, 2H, C10-H), 1.41 (s, 3H, C5-CH₃) and 1.16 (t, 3H, C7-CH₃CH₂NHCOO) ppm; CI-MS (CH₄), m/z: 264 (MH⁺), 246, 220, 193, 175, 149 and 72. Anal. (C₁₄H₁₇N O₄) C, H; N: Calcd. 5.32; Found 4.91.

(+)-(3aR)-3a-Methyl-2, 3,3a, 8a-Tetrahydrofuro[2,3-b] benzofuran-5yl N-ethyl carbamate (8b) and (+)-(5R)-5-Methyl-4, 5-dihydro-2, 5-methano-1, 3-benzodioxepin-7yl N-ethyl carbamate (11b)

Under a nitrogen atmosphere, two small pieces of sodium (about 1 mg) were added into a solution of mixture of **6b** and **7b** (26 mg, 0.135 mmol) in 5 mL of anhydrous ether at room temperature. The mixture was stirred for 2 minutes and, thereafter, ethyl isocyanate (32.8 μL, 0.408 mmol) was added to the reaction mixture in one portion. The reaction was continued for an hour at room temperature, 4.0 mL of water was then added and the ether layer was separated. After drying over sodium sulphate and filtering, the filtrate was evaporated to remove solvent. Thereafter, the residue was subjected to chromatography on silica gel plate (EtOAc/Hexane = 1/3) to afford products **8b** and **11b**. Product **8b** (14.8 mg, 83.1%): [α]$_D^{26}$ +92.5° (c=0.08, CHCl₃); e.e. 100%; ¹H-NMR (CDCl₃) δ 6.87-6.60 (m, 3H, Ar-H), 5.77 (s, 1H, C8a-H), 4.89 (s, br, 1H, NH), 4.06-3.56 (m, 2H, C2-H), 3.23 (m, 2H, C5-CH₂NHCOO), 2.13-1.91 (m, 2H, C3-H), 1.47 (s, 3H, C3a-CH₃) and 1.14 (t, 3H, C5-CH₃CH₂NHCOO) ppm; CI-MS (CH₄), m/z: 264 (MH⁺), 193, 175 and 72. Anal. (C₁₄H₁₇N O₄) C, H; N: Calcd. 5.32; Found 4.78. Product **11b** (10.4 mg, 58.4%): [α]$_D^{26}$ +10.0° (c=0.05, CHCl₃); e.e. 100%. ¹H-NMR (CDCl₃) δ 6.82-6,67(m, 3H, Ar-H), 5.69 (d, J=1.80Hz, 1H, C2-H), 4.88 (s, br, 1H, C7-NHCOO), 4.17, 3.70 (AB, J$_{gem}$=7.20Hz, 2H, C4-H), 3.22 (m, 2H, C-7CH₂NHCOO), 2.19-1.19 (m, 2H, C10-H), 1.41 (s, 3H, C5-CH₃) and 1.16 (t, 3H, C7-CH₃CH₂NHCOO) ppm; CI-MS (CH₄), m/z: 264 (MH⁺), 246, 220, 193, 175, 149 and 72. Anal. (C₁₄H₁₇N O₄) C, H, N.

(−)-(3aS)-3a-Methyl-2, 3,3a, 8a-Tetrahydrofuro[2,3-b] benzofuran-5yl N-o-tolyl carbamate (9a) and (+)-(5S)-5-Methyl-4, 5-dihydro-2, 5-methano-1, 3-benzodioxepin-7yl N-o-tolyl carbamate (12a)

Under a nitrogen atmosphere, two small pieces of sodium (about 1 mg) were added into a solution of mixture of **6a** and **7a** (27.9 mg, 0.145 mmol) in 5 mL of anhydrous ether at room temperature. The mixture was stirred for 2 minutes, and then o-tolyl isocyanate (18.9 μL, 0.149 mmol) was added to the mixture in one portion. The reaction was continued for 35 minutes at room temperature, 4 mL of water then was added and the ether layer was separated. After drying over sodium sulphate and filtering, the filtrate was evaporated to remove solvent. The residue was chromatographed on silica gel plate (EtOAc/Hexane = 1/3) to afford products **9a** and **12a**. Product **9a** (15.6 mg, 66.1%): [α]$_D^{27}$−103.0° (c=0.10, CHCl₃); e.e.100%; ¹H-NMR (CDCl₃) δ 7.84 (s, br, 1H, NH), 7.32-6.70 (m, 7H, Ar-H), 5.89 (s, 1H, C8a-H), 4.18-3.68 (m, 2H, C2-H), 2.39-2.05 (m, 2H, C3-H), 2.31 (s, 3H, Ar-CH₃) and 1.56 (s, 3H, C3a-CH₃) ppm; CI-MS (CH₄), m/z: 326 (MH⁺). Anal. (C₁₉H₁₉N O₄) H; Calcd. C, 70.14; N, 4.25; Found C, 69.18; N,3.71. Product **12a** (15.0 mg, 63.5%): [α]$_D^{27}$ +30.4° (c=0.135, CHCl₃), e.e. 100%; ¹H-NMR (CDCl₃) δ 7.87 (s, br, 1H, C7-NHCOO), 7.33-6.70 (m, 7H, Ar-H), 5.79 (d, J=1.80Hz, 1H, C2-H), 4.22, 3.79 (AB, J$_{gem}$=6.84Hz, 2H, C4-H), 2.37-2.01 (m, 2H, C10-H), 2.31 (s, 3H, Ar-CH₃) and 1.51 (s, 3H, C5-CH₃) ppm; CI-MS (CH₄), m/z: 326 (MH⁺). Anal. (C₁₉H₁₉N O₄) C; H: Calcd. 5.89; Found 6.36; N: Calcd. 4.31; Found 3.57.

(+)-(3a*R*)-3a-Methyl-2, 3,3a, 8a-Tetrahydrofuro[2,3-*b*] benzofuran-5yl *N-o*-tolyl carbamate (9b) and (−)-(5*R*)-5-Methyl-4, 5-dihydro-2, 5-methano-1, 3-benzodioxepin-7yl N-*o*-tolyl carbamate (12b)

Under a nitrogen atmosphere, two small pieces of sodium (about 1 mg) were added into a solution of mixture of **6b** and **7b** (18 mg, 0.09 mmol) in 5 mL of anhydrous ether at room temperature. The mixture was stirred for 2 minutes, and then *o*-tolyl isocyanate (18.3 µL, 0.145 mmol) was added in one portion. The reaction was continued for a further 35 minutes at room temperature, 4 mL of water then was added and the ether layer was separated. After drying over sodium sulphate and filtering, the filtrate was evaporated to remove solvent. The residue was chromatographed on silica gel plate (EtOAc/Hexane=1/3) to afford products **9b** and **12b**. Product **9b** (11.0 mg, 74.9%), $[\alpha]_D^{26}$+104.2° (c=0.095, CHCl$_3$); e.e. 100%; ^{1}H-NMR (CDCl$_3$) δ 7.84 (s, br, 1H, NH), 7.32-6.70 (m, 7H, Ar-H), 5.89 (s, 1H, C8a-H), 4.18-3.68 (m, 2H, C2-H), 2.39-2.05 (m, 2H, C3-H), 2.31 (s, 3H, Ar-CH$_3$) and 1.56 (s, 3H, C3a-CH$_3$) ppm; CI-MS (CH$_4$), m/z: 326 (MH$^+$). Anal. (C$_{19}$H$_{19}$N O$_4$) C, H; N: Calcd. 4.31; Found 3.78. Product **12b** (9.5 mg, 64.4%), $[\alpha]_D^{27}$−29.0° (c=0.10, CHCl$_3$); e.e. 100%; ^{1}H-NMR (CDCl$_3$) δ 7.87 (s, br, 1H, C7-NHCOO), 7.33-6.70 (m, 7H, Ar-H), 5.79 (d, J=1.80Hz, 1H, C2-H), 4.22, 3.79 (AB, J$_{gem}$=6.84Hz, 2H, C4-H), 2.37-2.01 (m, 2H, C10-H), 2.31 (s, 3H, Ar-CH$_3$) and 1.51 (s, 3H, C5-CH$_3$) ppm; CI-MS (CH$_4$), m/z: 326 (MH$^+$). Anal. (C$_{19}$H$_{19}$N O$_4$) N; Calcd. C, 70.14; N, 5.89; Found C, 69.49; N, 5.46.

(−)-(3a*S*)-3a-Methyl-2, 3,3a, 8a-Tetrahydrofuro[2,3-*b*] benzofuran-5yl N-*p*-isopropylphenyl carbamate (10a) and (+)-(5*S*)-5-Methyl-4, 5-dihydro-2, 5-methano-1, 3-benzodioxepin-7yl *N-p*-isopropylphenyl carbamate (13a)

Under a nitrogen atmosphere, two small pieces of sodium (about 1 mg) were added into a solution of mixture of **6a** and **7a** (16 mg, 0.083 mmol) in 5 mL of anhydrous ether at room temperature. The mixture was stirred for 2 minutes and *p*-isopropylphenyl isocyanate (14 µL, 0.086 mmol) was added to the mixture of **6a** and **7a** in one portion. The reaction was continued for an additional 45 minutes at room temperature; thereafter, 4 mL of water was added and the ether layer separated. After drying over sodium sulphate and filtering, the filtrate was evaporated to remove solvent. The residue was chromatographed on silica gel plate (EtOAc/ Hexane = 1/3) to afford products **10a** and **13a**. Product **10a** (8 mg, 54.4%): $[\alpha]_D^{26}$−91.4° (c=0.35, CHCl$_3$); e.e.100%; ^{1}H-NMR (CDCl$_3$) δ 7.31-6.71 (m, 8H, Ar-H, HNCOO), 5.80 (s, 1H, C8a-H), 4.09-3.59 (m, 2H, C2-H), 2.82 (septet, J=5.24Hz, 1H, CHMe$_2$), 2.19-1.96 (m, 2H, C3-H), 1.49 (s, 3H, C3a-CH$_3$) and 1.18 (d, J=5.24Hz, 6H, CH$_3$CCH$_3$) ppm; CI-MS (CH$_4$), m/z: 354 (MH$^+$). Anal. (C$_{21}$H$_{23}$N O$_4$) H; Calcd. C, 71.37; N, 3.94; Found C, 70.86; N, 3.30. Product **13a** (9 mg, 61.2%): $[\alpha]_D^{26}$ +50.0° (c=0.2, CHCl$_3$); e.e.100%; ^{1}H-NMR (CDCl$_3$) δ 7.30-6.72 (m, 8H, Ar-H, HNCOO), 5.71 (d, J=1.80Hz, 1H, C2-H), 4.17, 3.70 (AB, J$_{gem}$=5.40Hz, 2H, C4-H), 2.81 (septet, J=5.22 Hz, 1H, CHMe$_2$), 2.19-1.94 (m, 2H, C10-H), 1.48 (s, 3H, C5-CH$_3$) and 1.19 (d, J=5.22Hz, 6H, CH$_3$CCH$_3$) ppm; CI-MS (CH$_4$), m/z: 354 (MH$^+$). Anal. (C$_{21}$H$_{23}$N O$_4$) C, H; N: Calcd. 3.96; Found 4.56.

(+)-(3a*R*)-3a-Methyl-2, 3,3a, 8a-Tetrahydrofuro[2,3-*b*] benzofuran-5yl *N-p*-isopropylphenyl carbamate (10b) and (−)-(5R)-5-Methyl-4, 5-dihydro-2, 5-methano-1, 3-benzodioxepin-7yl *N-p*-isopropylphenyl carbamate (13b)

Under a nitrogen atmosphere, two small pieces of sodium (approx.1 mg) were added into a solution of mixture of **6b** and **7b** (18 mg, 0.094 mmol) in 5 mL of anhydrous ether at room temperature. The mixture was stirred for 2 minutes, and then *p*-isopropylphenyl isocyanate (14.6 µL, 0.096 mmol) was added in one portion. The reaction was continued for a further 45 minutes at room temperature, and then 4 mL of water was added and the ether layer separated. After drying over sodium sulphate and filtering, filtrate was evaporated to remove solvent. The residue was chromatographed on silica gel plate (EtOAc/Hexane = 1/3) to afford products

10b and **13b**. Product **10b** (13.7 mg, 82.1%): $[\alpha]_D^{27}$+91.4° (c=0.14, CHCl$_3$); e.e. 100%; ^{1}H-NMR (CDCl$_3$) δ 7.31-6.71 (m, 8H, Ar-H, HNCOO), 5.80 (s, 1H, C8a-H), 4.09-3.59 (m, 2H, C2-H), 2.82 (septet, J=5.24Hz, 1H, CHMe$_2$), 2.19-1.96 (m, 2H, C3-H), 1.49 (s, 3H, C3a-CH$_3$) and 1.18 (d, J=5.24Hz, 6H, CH$_3$CCH$_3$) ppm; CI-MS (CH$_4$), m/z: 354 (MH$^+$). Anal. (C$_{21}$H$_{23}$N O$_4$.1/8H$_2$O) C, H, N. Product **13b** (10.1 mg, 60.4%): $[\alpha]_D^{27}$−48.0° (c=0.1, CHCl$_3$); e.e. 100%; ^{1}H-NMR (CDCl$_3$) δ 7.30-6.72 (m, 8H, Ar-H, HNCOO), 5.72 (d, J=1.80Hz, 1H, C2-H), 4.17, 3.70 (AB, J$_{gem}$=5.40 Hz, 2H, C4-H), 2.81 (septet, J=5.22 Hz, 1H, CHMe$_2$), 2.19-1.94 (m, 2H, C10-H), 1.48 (s, 3H, C5-CH$_3$) and 1.19 (d, J=5.22Hz, 6H,CH$_3$CCH$_3$) ppm; CI-MS (CH$_4$), m/z: 354 (MH$^+$). Anal. (C$_{21}$H$_{23}$N O$_4$) H, N; C: Calcd. C 71.37; Found 70.75.

(+)-(3a*R*)-1,3a, 8-Trimethyl-1, 2,3,3a, 8,8a-hexahydropyrrolo[2,3-b] indol-5ol (14b)

Compound **14b** was synthesized, according to the procedure for its enantiomer, from N-methylphenetidine.[14]

(+)-(3a*R*)-1,3a, 8-Trimethyl-1, 2,3,3a, 8,8a-hexahydropyrrolo[2,3-b] indol-5yl *N*- (2'-methylphenyl) carbamate (17b)

Compound **17b** was made, according to the procedure for its antipode, from o-tolyl isocyanate and (+)-eseroline:[21] $[\alpha]_D^{26}$ +68.2 °(c=0.2, CHCl$_3$); ^{1}H NMR and MS were the same as reported for its enantiomer.[21] Anal. (C$_{21}$H$_{25}$N$_3$ O$_2$) H; Calcd. C, 71.70; N, 11.95; Found C, 70.08; N, 11.45.

(+)-(3a*R*)- 1, 3a, 8-Trimethyl-1, 2,3,3a, 8,8a-hexahydropyrrolo[2,3-b] indol-5yl *N*- (4'-isopropylphenyl) carbamate (18b)

Compound **18b** was synthesized, according to the procedure for its antipode, from *p*-isopropylphenyl isocyanate and (+)-eseroline:[21] $[\alpha]_D^{26}$+67.5 °(c=0.2, CHCl$_3$); ^{1}H NMR and MS were the same as reported for its enantiomer.[21] Anal. (C$_{23}$H$_{29}$N$_3$ O$_2$) H, N; C: Calcd. 72.79; Found 71.70.

(+)-(3a*R*)-3a, 8-Dimethyl-2, 3,3a, 8a-tetrahydrofuro[2,3-b] indol-5-ol (19b)

Compound **19b** made according to the procedure for synthesis of its enantiomer.[14, 17]

(+)-(3a*R*)-3a, 8-Dimethyl-2, 3,3a, 8a-tetrahydrofuro[2,3-b] indol-5-yl *N*- (2'-methylphenyl) carbamate (22b)

Compound **22b** was synthesized, according to the procedure for its antipode, from o-tolyl isocyanate and (+)-eseroline:[21] $[\alpha]_D^{26}$+27.5 °(c=0.2, CHCl$_3$); ^{1}H NMR and MS were the same as reported for its enantiomer.[20] Anal. (C$_{20}$H$_{22}$N$_2$ O$_3$) C, H; N: Calcd. 8.28; Found 7.84

(+)-(3a*R*)-3a, 8-Dimethyl-2, 3,3a, 8a-tetrahydrofuro[2,3-b] indol-5-yl *N*- (4'-isopropylphenyl) carbamate (23b)

Compound **23b** was made, according to the procedure for its antipode, from *p*-isopropylphenyl isocyanate and (+)-eseroline:[16] $[\alpha]_D^{26}$ +32.0 °(c=0.2, CHCl$_3$); ^{1}H NMR and MS were the same as reported for its enantiomer.[17] Anal. (C$_{22}$H$_{26}$N$_2$ O$_3$) C, H; N: Calcd. 7.64; Found 7.13.

X-ray Crystallography

A clear colorless crystal of dimensions $0.30 \times 0.23 \times 0.12$ mm^2 was mounted on glass fiber using a small amount of Epoxy. Data were collected on a Bruker three-circle platform diffractometer equipped with a SMART 6000 CCD detector. The crystals were irradiated using a rotating anode CuK$_\alpha$ source (λ = 1.54178) with incident beam Göbel mirrors. Data collection was performed and the unit cell was initially refined using *SMART*[v5.625].[53(a)] Data Reduction was performed using *SAINT* [v6.36A] [53(b)] and *XPREP* [v6.12].[53(c)] Corrections

were applied for Lorentz, polarization, and absorption effects using *SADABS* [v2.03].[53(d)] The structure was solved and refined with the aid of the programs in the *SHELXTL-plus* [v6.10] system of programs. [53(e)] The full-matrix least-squares refinement on F^2 included atomic coordinates and anisotropic thermal parameters for all non-H atoms. The H atoms were included using a riding model. The absolute configuration of C3 was established by making reference to unchanging chiral centers (C19, C21, and C24) in the synthetic procedure, with a resulting Flack parameter of −0.3(2). [53(f)] The X-ray data of compound **3** also can be found at the Cambridge Crystallographic Data Center (CCDC), <http://www.ccdc.cam.ac.uk/ >. The reference number of this crystal is 285734.

Quantitation of anticholinesterase activity

The action of enantiomers **8**–**13** and compounds **17b**, **18b**, **22b** and **23b** to inhibit the ability of freshly prepared human AChE and BChE to enzymatically degrade their respective specific substrates, acetyl-(β-methyl)thiocholine and *s*-butyrylthiocholine (0.5 mmol/L) (Sigma Chemical Co., St. Lois, MO), was quantified.[13–17, 19–21] Samples of AChE and BChE were derived from freshly collected human whole red blood cells and plasma, respectively. Compounds were dissolved in *Tween 80*/EtOH 3:1 (*v:v*; <150 μL total volume) and were diluted in 0.1 M Na_3PO_4 buffer (pH 8.0) in half-log concentrations to provide a final concentration range that spanned 0.3 nM to 30 uM. *Tween 80*/EtOH was diluted to in excess of 1 in 5000. No inhibitory action on either AChE or BChE was detected in separate experiments where the ChEI activity of the known compound **15a** was quantified in excess and without *Tween 80*/EtOH.

For the preparation of BChE, freshly collected blood was centrifuged (10,000 *g*, 10 min, 4° C) and plasma was removed and diluted 1:125 with 0.1 M Na_3PO_4 buffer (pH 7.4). Plasma was carefully checked to insure an absence of haemolysis. For AChE preparation, erythrocytes were washed five times in isotonic saline, lysed in 9 volumes of 0.1 M Na_3PO_4 buffer (pH 7.4) containing 0.5% *Triton-X* (Sigma) and then were diluted with an additional 19 volumes of buffer to a final dilution of 1:200.

Analysis of anticholinesterase activity was undertaken by utilizing a 25 μL sample of each enzyme preparation, and was undertaken at their optimal working pH, 8.0, in 0.1 M Na_3PO_4 buffer (0.75 mL total volume). Compounds were preincubated with enzymes (30 min, at room temperature) and then were incubated with their respective substrates and with 5,5'-dithiobis-2-nitrobenzoic acid (25 min, 37° C). The substrate/enzyme interaction was immediately halted by the addition of excess enzyme inhibitor (physostigmine 1×10^{-5} M) and production of a yellow thionitrobenzoate anion was then measured by spectrophotometer at 412 nm λ. To correct for nonspecific substrate hydrolysis, aliquots were co-incubated under conditions of absolute enzyme inhibition (by the addition of 1×10^{-5} M physostigmine (**15a**)), and the associated alteration in absorbance was subtracted from that observed through the concentration range of each test compound. Each agent was analyzed on four separate occasions and assayed along-side physostigmine (**15a**), as a control and external standard whose activity we have previously reported. [13–17, 19–21] The mean enzyme activity at each concentration of test compound was then expressed as a percent of the activity in the absence of compound. This was transformed into a logit format (where logit = ln(%activity/100 minus %activity)) and then was plotted as a function of its log concentration. Inhibitory activity was calculated as an IC_{50}, defined as the concentration of compound (nM) required to inhibit 50% of enzymatic activity, which was determined from a correlation between log concentration and logit activity. Only results obtained from correlation coefficients of $r^2 \geq -0.98$ were considered acceptable. Studies that did not obtain this threshold were repeated.

Computer Aided Molecular Modeling

Computer aided molecular modeling was undertaken using Sybyl version 7.0 (Tripos Inc., St. Louis, MO). The numbering of the amino acid residues is based on that for *Tc*AChE. Molecular volume calculations were performed by using multiple volume comparison routine. The atomic coordinates of the transition state of *Tc*AChE were obtained from the protein data bank (PDB entry: 1AMN)[38], and were used for transition state studies. In undertaking this, i) molecules of water were removed, ii) the small molecule, m- (*N, N, N*-trimethylammonio)-2,2,2-trifluoroacetophenone (TMTFA), was extracted and, iii), the carbonyl carbon of TMTFA was retained in the tetrahedral conformation. iv) The carbonyl carbon of the inhibitor, (−)-(3a*S*)-N-2'-methylphenyl carbamoyl phenol of furobenzofuran (**9a**), was modified into the tetrahedral conformation and then superimposed with that of TMTFA, keeping both phenyl groups on the same side and, as much as possible, in a superimposed conformation. Thereafter, compound **9a** was merged into the active domain of *Tc*AChE. The covalent bond between carbonyl carbon of compound **9a** and γ-O of Ser_{200} was created. To maintain the hydrogen bonds associated with acylation, the distances between the NH of Gly_{118}, Gly_{119}, Ala_{201} and oxygen of the ligand carbonyl, γ-O of Ser_{200} and a single H, the hydrogen and N of His_{440}, the NH of His_{440} and oxygen of Glu_{327} were constrained. All the residues outside a radius of 10 Å from the compound **9a** were aggregated. The energy of the enzyme-inhibitor complex was minimized with the conjugate gradient algorithm.

Supplementary Material

Refer to Web version on PubMed Central for supplementary material.

Acknowledgement

REFERENCE

1. Drachman DA, Leavitt J. Human memory and the cholinergic system. A relationship to aging? Arch Neurol 1974;30:113–121. [PubMed: 4359364]

2. Small DH. Do acetylcholinesterase inhibitors boost synaptic scaling in Alzheimer's disease? Trends Neurosci 2004;27:245–249. [PubMed: 15111005]

3. Lahiri DK, Rogers JT, Sambamurti K, Greig NH. Rationale for the development of cholinesterase inhibitors as anti-Alzheimer agents. Curr Pharm Des 2004;10:3111–3119. [PubMed: 15544501]

4. Cummings JL. Cholinesterase inhibitors: A new class of psychotropic compounds. Am J Psychiatry 2000;157:4–15. [PubMed: 10618007]

5. Courtney C, Farrell D, Gray R, Hills R, Lynch L, Sellwood E, Edwards S, Hardyman W, Raftery J, Crome P, Lendon C, Shaw H, Bentham P. AD2000 Collaborative Group. Long-term donepezil treatment in 565 patients with Alzheimer's disease (AD2000): randomised double-blind trial. Lancet 2004;363(9427):2105–2115. [PubMed: 15220031]

6. Lopez OL, Becker JT, Saxton J, Sweet RA, Klunk W, DeKosky ST. Alteration of a clinically meaningful outcome in the natural history of Alzheimer's disease by cholinesterase inhibition. J Am Geriatr Soc 2005;53:83–87. [PubMed: 15667381]

7. Conworth, E. The Alkaloids. Manskel, RHF., editor. Vol. 8. New York: Academic; 1965. p. 27-46.

8. Robinson, B. The Alkaloids. Manskel, RHF., editor. Vol. 10. New York: Academic; 1967. p. 383-401.and 1971, Vol.13, pp 213 – 226

9. Brossi A. Bioactive Alkaloids. 4. Results of Recent Investigations with Colchicine and Physostigmine. J. Med. Chem 1990;33:2311–2319. [PubMed: 2202827]

10. Greig NH, Pei XF, Soncrant TT, Ingram DK, Brossi A. Phenserine and Ring C Hetero-Analogues: Drug Candidates for Treatment of Alzheimer's Disease. Med. Res. Rev 1995;15:3–31. [PubMed: 7898167]

11. Greig NH, Sambamurti K, Yu QS, Brossi A, Bruinsma G, Lahiri DK. An overview of phenserine tartrate, a novel acetylcholinesterase inhibitor for the treatment of Alzheimer's disease. Cur. Alz. Res 2005;2:281–291.

12. Greig, NH.; Sambamurti, K.; Yu, QS.; Perry, TA.; Holloway, HW.; Haberman, F.; Brossi, A.; Ingram, DK.; Lahiri, DK. Butyrylcholinesterase: its selective inhibition and relevance to Alzheimer's disease. In: Giacobini, E., editor. Butyrylcholinesterase: Its Function and Inhibition. London: Martin Dunitz Ltd.; 2003. p. 69-90.

13. Pei XF, Greig NH, Bi S, Broosi A, Toome V. Inhibition of Human Acetylcholinesterase by Unnatural (+)-(3aR)-N1-Norphysostigmine and Arylcarbamate analogues. Med. Chem. Res 1995;5:265–270.

14. Yu QS, Luo W, Holloway HW, Utsuki T, Perry TA, Lahiri DK, Greig NH, Brossi A. Racemic N^1-Norphenserine and Its Enantiomers: Unpredicted Inhibition of Human Acetyl- and Butylylcholinesterase and β-Amyloid Precursor Protein *in vitro Heterocycles* 2003;619:529–539.

15. Yu QS, Liu C, Brzostowska M, Chrisey L, Brossi A, Greig NH. Physovenines: Efficient Synthesis of (−)- and (+)-Physovenine and Synthesis of Carbamate Analogues of (−)-Physovenine. Anticholinesterase Activity and Analgesic Properties of Optically Active Physovenines. Helvetica Chimica Acta 1991;74:761–766.

16. Brzostowska M, He XS, Greig NH, Rapoport S, Brossi A. Phenylcarbamates of (−)- Eceroline and (−)-Physovenol: Selective Inhibition of Acetyl and, or Butyrylcholinesterases by Phenylcarbamates. Med. Chem. Res 1992;2:238–246.

17. Luo W, Yu QS, Zhan M, Parrish D, Deschamps JR, Kulkarrni SS, Holloway HW, Alley GM, Lahiri DK, Brossi A, Greig NH. Novel Acetylcholinesterase based on the Molecular Skeletons of Furobenzofuran and Methanobenzodioxepine. J. Med. Chem 2005;48:986–994. [PubMed: 15715468]

18. Luo W, Yu QS, Holloway HW, Parrish DA, Greig NG, Brossi A. Syntheses of Tetrahydrofurobenzofurans and Dihydro-methanobenzodioxepines from 5-Hydroxy-3-methyl-3*H*-benzofuran-2-one. Rearrangement and Ring Expansion under Reductive Conditions on Treatment with Hydrides. J. Org. Chem 2005;70:6171–6176. [PubMed: 16050674]

19. Yu QS, Holloway HW, Utsuki T, Brossi A, Greig NH. Phenserine-based synthesis of novel selective inhibitors of butyrylcholinesterase for Alzheimer's disease. J. Med. Chem 1999;42:1855–1861. [PubMed: 10346939]

20. Yu QS, Zhu X, Holloway HW, Whittaker NF, Utsuki T, Brossi A, Greig NH. Anticholinesterase activity of compounds related to geneserine tautomers – N-oxides and 1,2-oxazines. J. Med. Chem 2002;45:3684–3691. [PubMed: 12166941]

21. Yu QS, Holloway HW, Flippen-Anderson F, Hoffman B, Brossi A, Greig NH. Methyl analogues of the experimental Alzheimer drug, phenserine: synthesis and structure/activity relationships for acetyl- and butyrylcholinesterase inhibitory action. J. Med. Chem 2001;44:4062–4071. [PubMed: 11708910]

22. Kamal MA, Greig NH, Alhomida AS, Al-Jafari AA. Human acetylcholinesterase inhibition kinetics of the experimental Alzheimer therapeutic, tolserine. Biochem. Pharmacol 2000;60:561–570. [PubMed: 10874131]

23. Al-Jafari AA, Kamal MA, Alhomida AS, Greig NH. Brain acetylcholinesterase inhibition kinetics of two experimental Alzheimer's disease drugs, phenserine and tolserine, in the rat. J.Biochem. Mol. Biol. & Biophys 2000;4:323–335.

24. Kamal MA, Al-Jafari AA, Greig NH. A new, simple and economical approach to analyze the inhibition kinetics of the enzyme, acetylcholinesterase, by using the experimental Alzheimer drug, tolserine. Emir. Med. J 2002;20:333–337.

25. Marshall, GR.; Barry, CD. Abstr. Am. Cryst. Assoc. Honolulu, HI: 1979. Functional Representation of Molecular Volume for Computer-Aided Drug Design.

26. Sufrin JR, Dunn DA, Marshall GR. Steric Mapping of The L-Methionine Binding Site of ATP:L-Methionine *S*-Adenosyltransferase. Molecular Pharmacology 1981;19:307–313. [PubMed: 7231391]

27. Brufani, M.; Filocamo, L. Rational design of cholinesterase inhibitors. In: Giacobini, E., editor. Cholinesterases and Cholinesterase Inhibitors. London: Martin Dunitz Ltd.; 2000. p. 27-46.

28. Reiner, E.; Radic, Z. Mechanism of action of cholinesterase inhibitors. In: Giacobini, E., editor. Cholinesterases and Cholinesterase Inhibitors. London: Martin Dunitz Ltd.; 2000. p. 27103-27119.

29. Greenblatt HM, Dvir H, Silman I, Sussman JL. Acetylcholinesterase: a multifaceted target for structure-based drug design of anticholinesterase agents for the treatment of Alzheimer's disease. J Mol Neurosci 2003;20:369–383. [PubMed: 14501022]

30. Krasiski A, Radi Z, Manetsch R, Raushel J, Taylor P, Sharpless KB, Kolb HC. In Situ Selection of Lead Compounds by Click Chemistry Target-Guided Optimization of Acetylcholinesterase Inhibitors. J. Am. Chem. Soc 2005;127:6686–6692. [PubMed: 15869290]

31. Muñoz-Ruiz P, Rubio L, García-Palomero E, Dorronsoro I, Monte-Millán M, Valenzuela R, Usán P, Austra C, Bartolini M, Andrisano V, Bidon-Chanal A, Orozco M, Luque FJ, Medina M, Martínez A. Design, synthesis and biological evaluation of dual binding site acetylcholinesterase inhibitors: new disease modifying agents for Alzheimer's disease. J. Med. Chem. 2005E-online Oct.

32. Otoguro K, Kuno F, Omura S. Arisugacins, selective acetylcholinesterase inhibitors of microbial origin. Pharmacol Ther 1997;76:45–54. [PubMed: 9535168]

33. Soreq H, Seidman S. Acetylcholinesterase--new roles for an old actor. Nat Rev Neurosci 2001;2:294–302. [PubMed: 11283752]

34. Massoulie, J. Molecular forms and anchoring of acetylcholinesterase. In: Giacobini, E., editor. Cholinesterases and Cholinesterase Inhibitors. London: Martin Dunitz Ltd.; 2000. p. 81-102.

35. Soreq H, Gnatt A, Loewenstein Y, Neville LF. Excavations into the active-site gorge of cholinesterases. Trends Biochem Sci 1992;17:353–358. [PubMed: 1412713]

36. Dvir H, Wong DM, Harel M, Barril X, Orozco M, Luque FJ, Munoz-Torrero D, Camps P, Rosenberry TL, Silman I, Sussman JL. 3D structure of *Torpedo californica* acetylcholinesterase complexed with huprine X at 2.1 A resolution: kinetic and molecular dynamic correlates. Biochemistry 2002;41:2970–2981. [PubMed: 11863435]

37. Silman I, Millard CB, Ordentlich A, Greenblatt HM, Harel M, Barak D, Shafferman A, Sussman JL. A preliminary comparison of structural models for catalytic intermediates of acetylcholinesterase. Chem Biol Interact 1999;119(120):43–52. [PubMed: 10421437]

38. Silman I, Harel M, Axelsen P, Raves M, Sussman JL. Three-dimensional structures of acetylcholinesterase and of its complexes with anticholinesterase agents. Biochem Soc Trans 1994;22:745–749. [PubMed: 7821677]

39. Nachon F, Asojo OA, Borgstahl GEO, Masson P, Lockridge O. Role of waterin aging of human butylcholinesterase inhibited by echothiophate: the crystal structure suggest two alternative mechanisms of aging. Biochemistry 2005;44:1154. [PubMed: 15667209](PDB codes: 1XLW, 1XLV, 1XLU)

40. Nicolet Y, Lockridg O, Masson P, Fontecilla-Camps JC, Nachon F. Crystal Structure of Human Butyrylcholinesterase and of its Complexes with Substrate and Products. J. Biol. Chem 2003;278:41141. [PubMed: 12869558](PDB codes: 1PO1, 1POM, 1POP, 1POQ)

41. Nachon F, Nicolet Y, Viguié N, Masson P, Fontecilla-Camps JC, Lockridg O. Engineering of a monomeric and low-glycosylated form of human butyrylcholinrsterase: exprassion, purification, characterization and crystallization. Eur. J. Biochem 2002;269:630. [PubMed: 11856322]

42. Inestrosa NC, Sagal JP, Colombres M. Acetylcholinesterase interaction with Alzheimer amyloid beta. Subcell Biochem 2005;38:299–317. [PubMed: 15709485]

43. Porschke D, Creminon C, Cousin X, Bon C, Sussman JL, Silman I. Electrooptical measurements demonstrate a large permanent dipole moment associated with acetylcholinesterase. Biophys J 1996;4:1603–1608. [PubMed: 8785319]

44. Felder CE, Botti SA, Lifson S, Silman I, Sussman JL. External and internal electrostatic potentials of cholinesterase models. J Mol Graph Model 1997;15:318–327. [PubMed: 9640563]335-7

45. Scowen, RL. Transition States of Biochemical Processes. Gandour, RD.; Schowen, RL., editors. New York: Plenum; 1978. p. 555-578.

46. Harel M, Quinn DQ, Nair HK, Silman I, Sussman JL. The X –ray Structure of a Transition State Analog Complex Reveals the Molecular Origins of the Catalytic Power and Substrate Specificity of Acetylcholinesterase. J Am Chem Soc 1996;118:2340–2346.

47. Perola E, Cellai L, Lamba D, Filocamo L, Brufani M. long Chain Analogs of Physostigmine as Potential Drugs for Alzheimer's Disease: new Insights Into the Mechanism of Action in the Inhibition of Acetylcholinesterase. Biochemistry.Biophys. Acta 1997;1343:41.

48. Bartolucci C, Perola E, Cellai L, Brufani M, Lamba D. "Back Door" Opening Implied by the Crystal Structure of Carbamoylated Acetylcholinesterase. Biochemistry 1999;38:5714. [PubMed: 10231521]

49. Koellner G, Steiner T, Millard CB, Silman I, Sussuman JL. A Neutral Molecule in Cation-binding Site: Specific Binding of a PEG-SH to Acetylcholinesterase from *Torpedo californica*. J. Mol. Biol 2002;320:721–725. [PubMed: 12095250]

50. Yu QS, Greig NH, Holloway HW, Brossi A. 4'-Hyroxyphenylcarbamates of (3aS)-eseroline and (3aS)-N(1)-noreseroline: potential metabolites of the Alzheimer's anticholinesterase drug phenserine. Heterocycles 1999;50:95–102.

51. Francis PT, Nordberg A, Arnold SE. A preclinical view of cholinesterase inhibitors in neuroprotection: do they provide more than symptomatic benefits in Alzheimer's disease? Trends Pharmacol Sci 2005;26:104–111. [PubMed: 15681028]

52. Hashimoto M, Kazui H, Matsumoto K, Nakano Y, Yasuda M, Mori E. Does donepezil treatment slow the progression of hippocampal atrophy in patients with Alzheimer's disease? Am J Psychiatry 2005;162:676–682. [PubMed: 15800138]

53. Bruker. SMART v5.625. Madison, Wisconsin, USA: Bruker AXS Inc.; 2001a. Bruker. SAINT v6.36A. Madison, Wisconsin, USA: Bruker AXS Inc.; 2002. Bruker. XPREP v6.12. Madison, Wisconsin, USA: Bruker AXS Inc.; 2001b. Bruker. SADABS v2.03. Madison, Wisconsin, USA: Bruker AXS Inc.; 2000. Bruker. SHELXTL v6.10. Madison, Wisconsin, USA: Bruker AXS Inc.; 2000. (f) Flack HD. Acta Cryst 1983;A39:876–881.
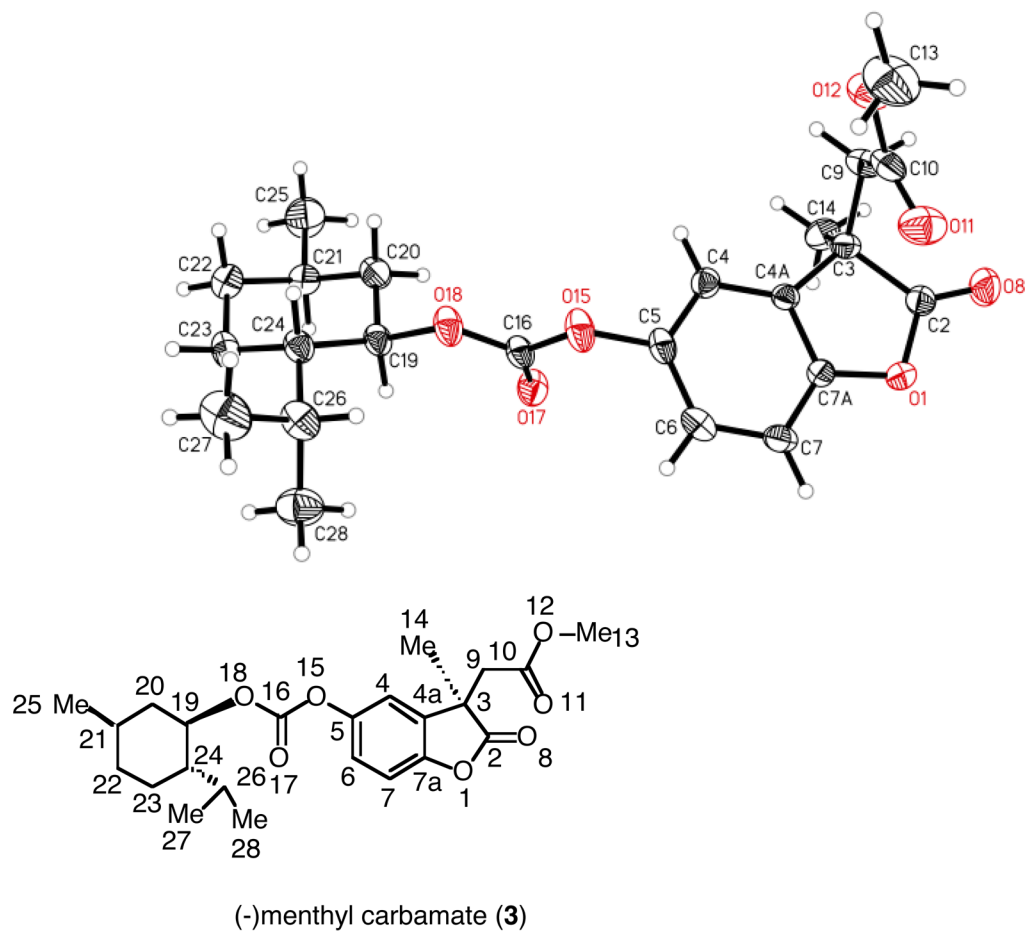
Figure 1.
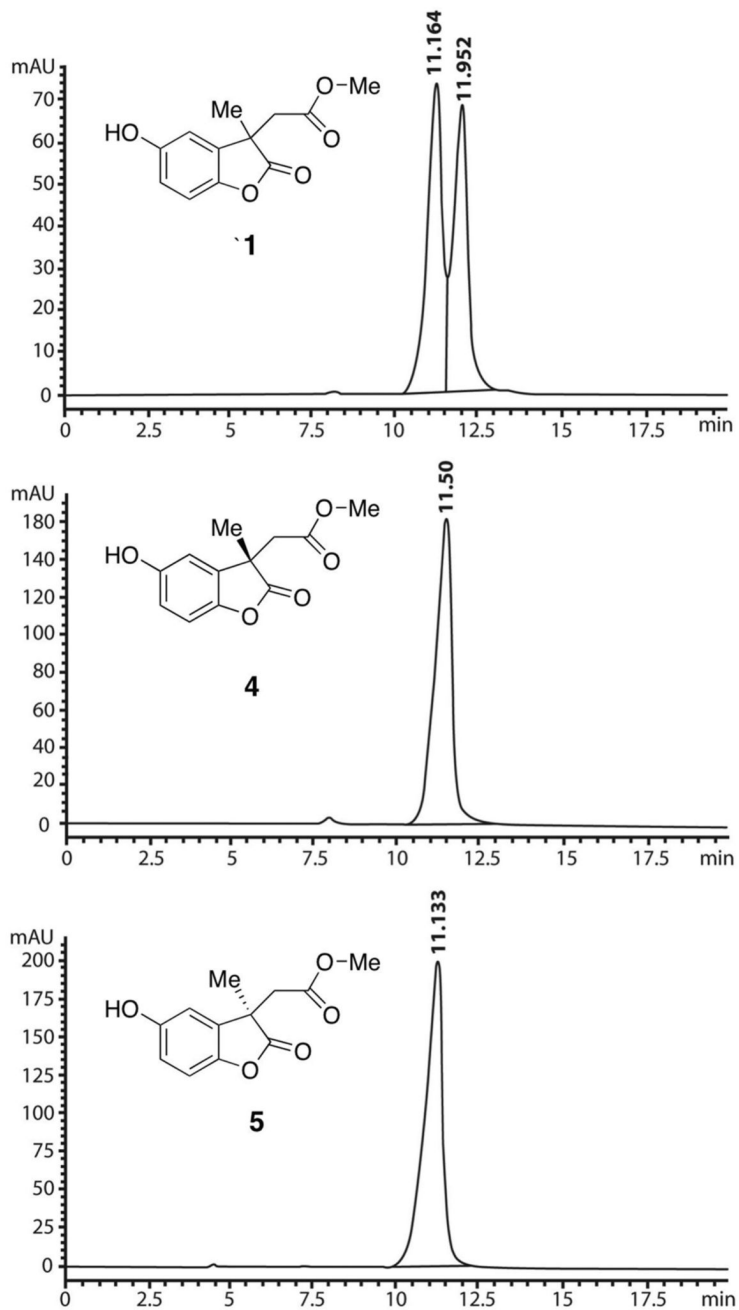X-ray crystallographic picture and corresponding chemical structure of 3

Figure 2.
Chiral HPLC analysisa of compounds **1**, **4** and **5**
[a] Instrument: HP1100; column: ChiraDex 5 µm; Flow-rate: 0.5 ml/min; Detection: UV 254 nm; Elutent: MeOH/H2O 45/55; Temperature: r.t. (Retention times, **1**: 11.164 and 11.952 min; **4**: 11.50 min; 5: 11.133 min).
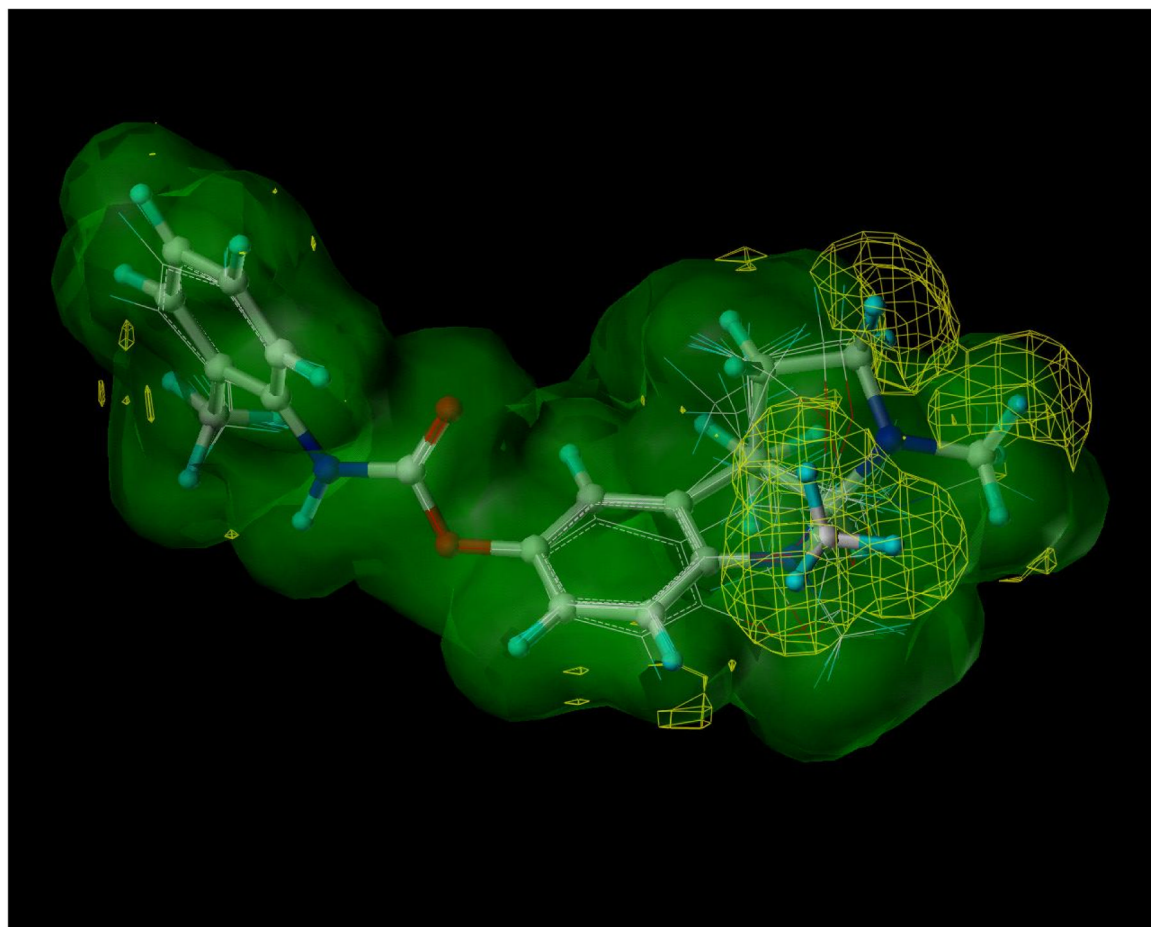
Figure 3.
The union of molecular volume maps for the four active, *S*-configuration compounds **9a**, **12a**, **17a**, **22a** (green area) provide the enzyme-excluded volume. The molecular volume map of compound **17b** minus the enzyme-excluded volume is the estimate extra volume of **17b** (yellow meshed area)
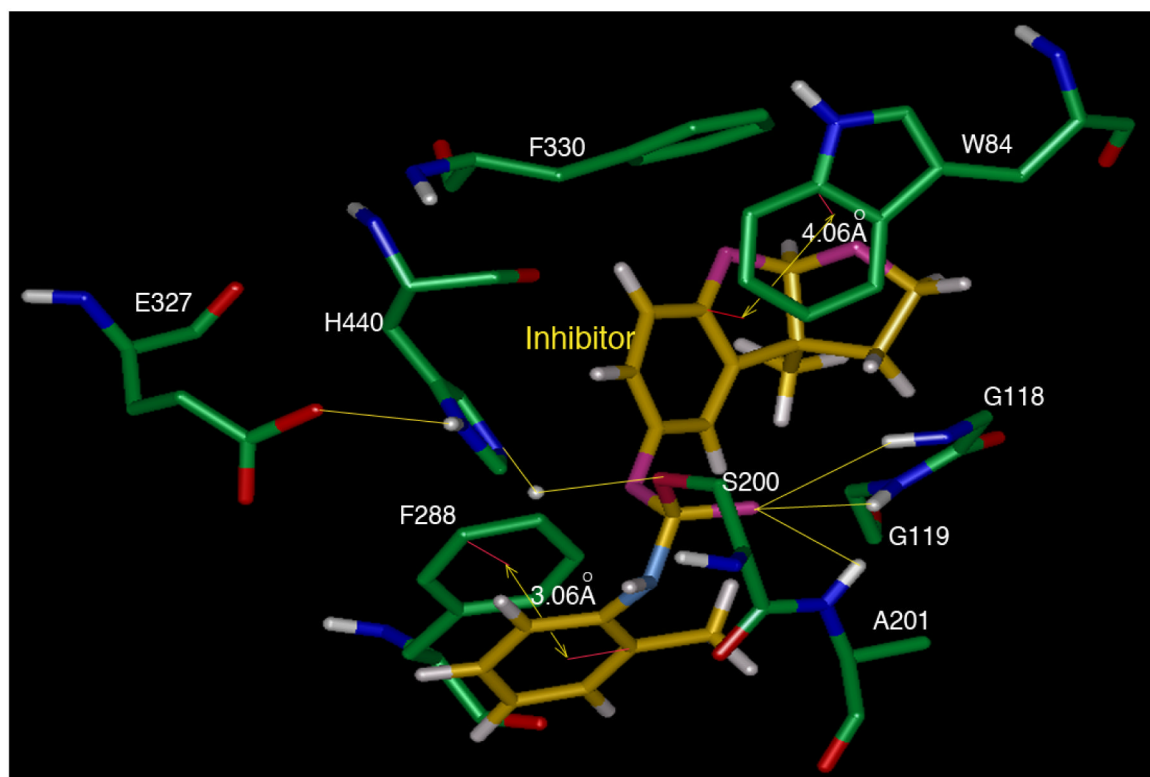
Figure 4.
Close-up of compound **9a** – *Tc*AChE complex showing its covalent bonding with Ser_{200}. The yellow lines denote hydrogen bond to the residues in the oxyanion hole, i.e. Gly_{118}, Gly_{119}, and Ala_{201}, and in the catalytic triad, Ser_{200}, His_{440}, and Glu_{327}.

26 $R_1 =$ [phenyl propyl group] $R_2 =$ [1-(4-methylphenyl)-1-methylethyl group]

27 $R_1 = -CH_3$ $R_2 =$ [benzyloxy-4-methylphenyl group]

Figure 5.

Donepezil (*Aricept*)

Huperzine A

Rivastigmine (*Exelon*)

Galantamine (*Reminyl*)

(-)-Phenserine

Tacrine (Cognex)
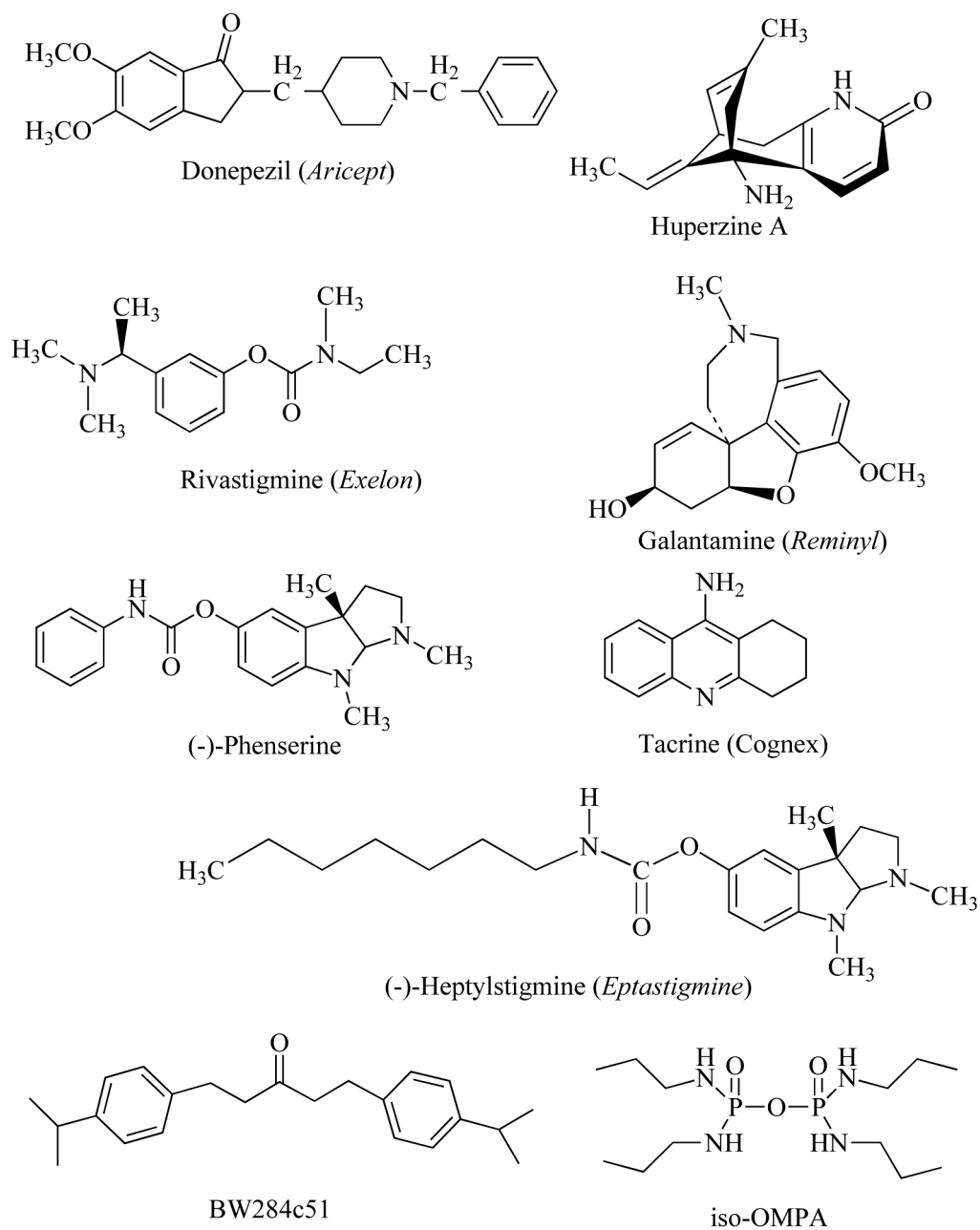
(-)-Heptylstigmine (*Eptastigmine*)
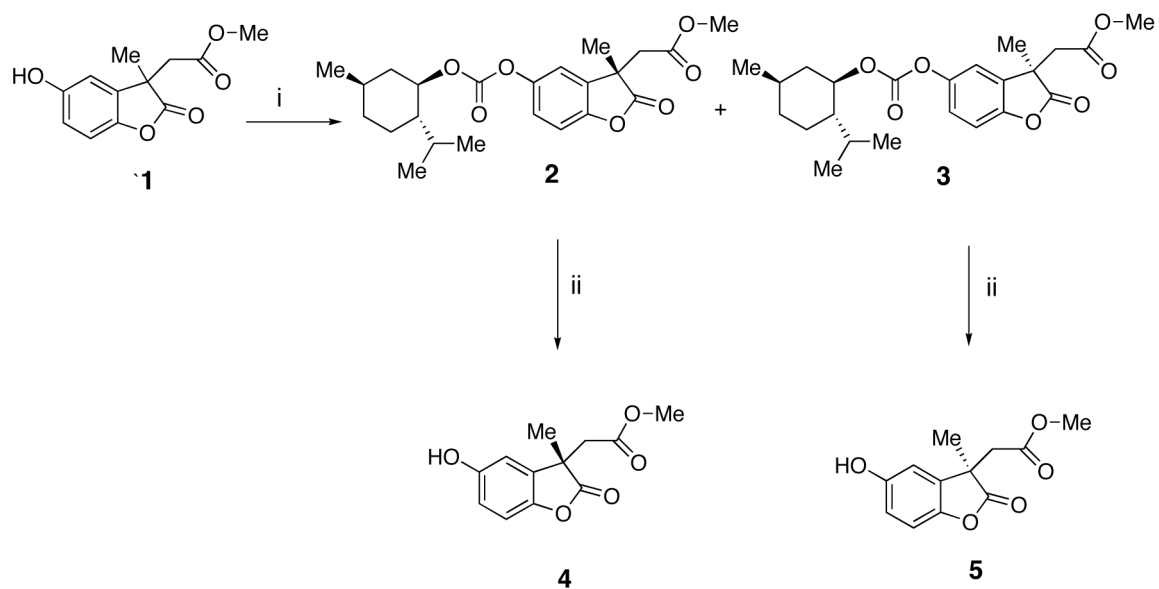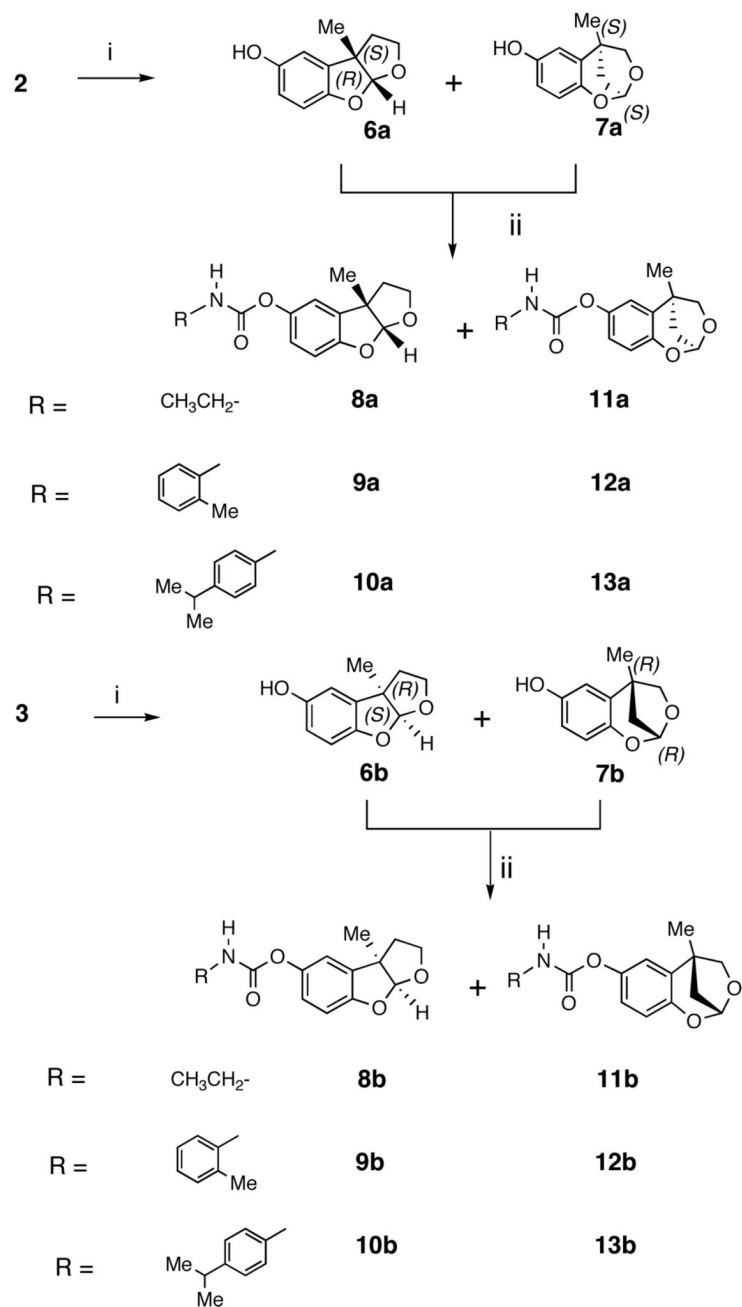
BW284c51

iso-OMPA
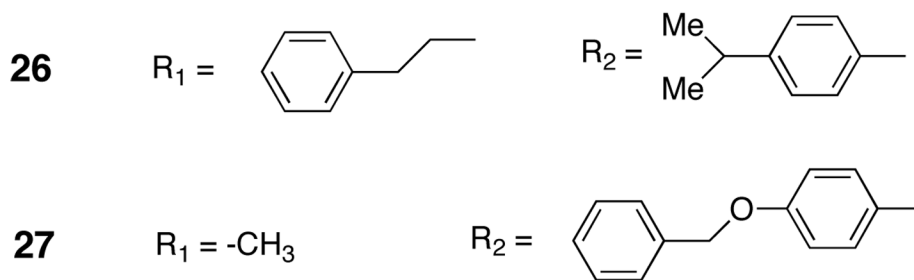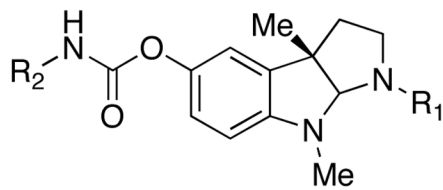
Figure 6.
Chemical structures of clinically relevant cholinesterase inhibitors (Table 2)
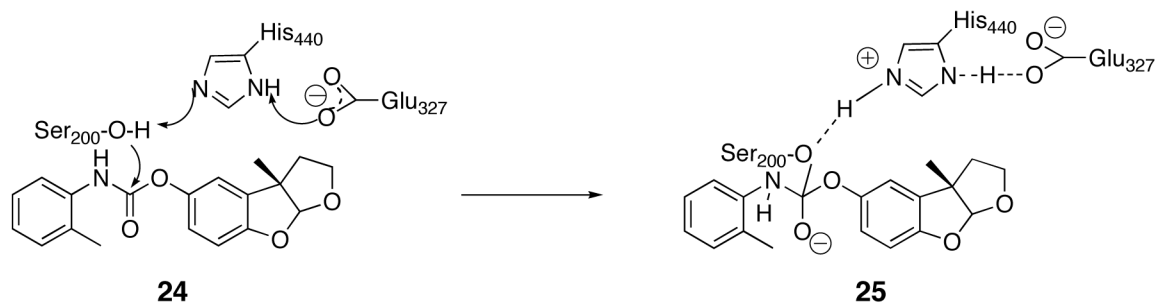
Scheme 1.
i) a, (−)-Menthy chloroformate, Et$_3$N, benzen,N$_2$, r.t., 1.5 hrs; b, recrystallized several times in hexane, then in ethanol. ii) a, NaOH, MeOH, r.t., 1.5 hrs; b, r.t. 1N HCl

Scheme 2.
i) a. LAH/Et$_2$O, r.t., 1 hr; b. 1M HCl in Et$_2$O, r.t., 0.5 hr. ii) Na, RNCO/Et2O, r.t., 0.5–1.0 hr.
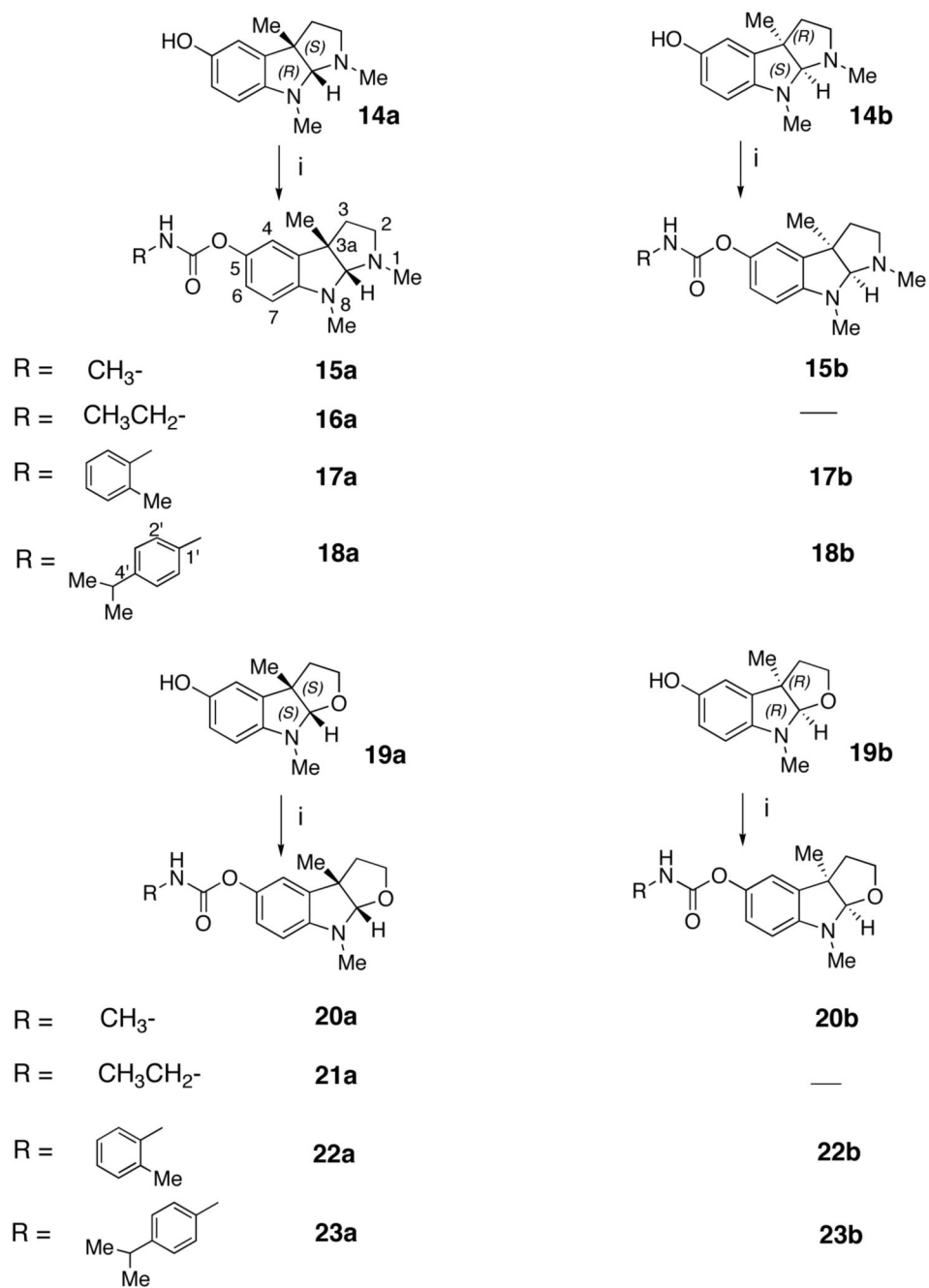
Scheme 3.
i) Na, RNCO/Et₂O, r.t.

Scheme 4.

Table 1

50% Inhibitory Concentration (IC$_{50}$, nM, ± SEM) of Compounds Versus Freshly Prepared Human Erythrocyte AChE and Plasma BChE

No.	Compounds	AChE(IC$_{50}$,nM)	R/S*	BChE(IC$_{50}$,nM)	R/S*	A/B$
Carbamates of tetrahydrofurobenzofuran						
8a	(−)-(3aS)-ethyl-	100±34		3±1		33-BChE
8b	(+)-(3aR)-ethyl-	486±63	4.8	28±1	9.3	17-BChE
9a	(−)-(3aS)-2'-methylphenyl-	20±1		11,400±1300		570-AChE
9b	(+)-(3aR)-2'-methylphenyl-	36±1	1.8	36,400±4750	3.2	1000-AChE
10a	(−)-(3aS)-4'-isopropylphenyl-	None#				>2300-BChE
10b	(+)-(3aR)- 4'-isopropylphenyl-	6,700±1750	13±5	40±2	3.1	167-BChE
Carbamates of benzodioxepine						
11a	(−)-(5S)-ethyl-	610±106		23±5		27-BChE
11b	(+)-(5R)-ethyl-	2420±213	4.0	120±66	5.3	20-BChE
12a	(+)-(5S) -2'-methylphenyl-	38±1.0		52,000±10,000		1350-AChE
12b	(−)-(5R)-2'-methylphenyl-	97±4	2.6	None#		>310-AChE
13a	(+)-(5S)-4'-isopropylphenyl-	None#		15±1.5		>2000-BChE
13b	(−)-(5R)- 4'-isopropylphenyl-	3430±145	3.5	54±11	3.5	64-BChE
Carbamates of physostigmine						
15a	(−)-(3aS)-methyl-	28±2		16±3		2-BChE
15b	(+)-(3aR)-methyl-	9890±9	353	2490±290	155	4-BChE
16a	(−)-(3aS)-ethyl-	94±12		4±1		24-BChE
—	(+)-(3aR)-ethyl-	Not synthesized				
17a	(−)-(3aS) -2'-methylphenyl-	10±2		1950±240		195-AChE
17b	(+)-(3aR)-2'-methylphenyl-	5510±190	551	1180±450	0.6	5-BChE
18a	(−)-(3aS)-4'-isopropylphenyl-	760±20		50±1		15-BChE
18b	(+)-(3aR)-4'-isopropylphenyl-	None#	5100±575	102	>6-BChE	
Carbamates of physovenine**						
20a	(−)-(3aS)-methyl-	27±1		4±1		7-BChE
20b	(+)-(3aR)-methyl-	56±1	2.1	56±15	14	none
21a	(−)-(3aS)-ethyl-	82±4		2±0		40-BChE
—	(+)-(3aR)-ethyl ethyl carbamate	Not synthesized				
22a	(−)-(3aS) -2'-methylphenyl-	13±1		1560±120		120-AChE
22b	(+)-(3aR)-2'-methylphenyl-	142±135	11	5100±1780	3.3	6-AChE
23a	(−)-(3aS)-4'-isopropylphenyl-	3860±970		17±2		225-BChE
23b	(+)-(3aR)- 4'-isopropylphenyl-	None#		23±2	1.4	>1300-BChE

* R/S IC$_{50}$ of R-configuration/ IC$_{50}$ of S-configuration.

$ A/B: selectivity for AChE or BChE from IC$_{50}$ values.

** The IC$_{50}$ data of compounds **15a**, **15b** are from reference 14, the data of compounds **20a**, **23a,20b** are from reference 15, the data of **17a**, **22a**, **18a** are from reference 16, and the data of **16a**, **21a** are from reference 17. In each case, however, enzyme was obtained from the same individual and assays were performed similarly. #None: Insufficient activity in the range of 0.3 nM to 30 uM to calculate an IC$_{50}$ value, and hence considered to be inactive.

Table 2

Comparison of the IC_{50} Values (± SEM) of Approved ChEIs of Clinical Interest Versus Freshly Prepared Human Erythrocyte AChE and Plasma BChE (Figure 6)

Compound	IC_{50} Value[*] (nM)		Selectivity
	AChE	BChE	
Tacrine	190 ± 40	47 ± 10	4-BChE
Donepezil	22 ± 8	4150 ± 1700	188-AChE
Rivastigmine	4150 ± 160	37 ± 5	122-BChE
Galanthamine	800 ± 60	7300 ± 830	9-AChE
(−)-Phenserine	22 ± 1.4	1560 ± 45	70-AChE
(−)-(3a*S*)-phenylcarbamate of physostigmine			
Heptylstigmine	22 ± 2	5.0 ± 0.1	4-BChE
(−)-(3a*S*)-heptylcarbamate of physostigmine			
Huperzine A	47 ± 22	>10,000	>212-AChE
BW284c51[#]	18 ± 8	48,000	2660-AChE
Iso-OMPA[#]	340,000	980 ± 550	35-BChE

[*] IC_{50} values were determined in duplicate on a minimum of 4 different occasions from enzyme collected from the same individual as assays described for Table 1.

[#] BW284c51 (1,5-bis(4-allyldimethylammoniumphenyl)pentan-3-one dibromide) and Iso-OMPA (tetra(monoisopropyl)pyrophosphortetramide) are classical selective inhibitors of AChE and BChE, respectively

Table 3

Estimate Extra Volume[*] and the Ratio of Anticholinesterase Activity *R/S*

No.	Compounds	Estimate Extra Volume ($\AA^3$)	*R/S*(AChE)
9b	Tetrahydrofurobenzofuran series (+)-(3a*R*)-2'-methylphenylcarbamate	7.1	1.8
12b	Dihydrobenzodioxepine series (−)-(5*R*)-2'-methylphenylcarbamate	19.9	2.6
17b	Physostigmine series (+)-(3a*R*)-2'-methylphenylcarbamate	24.8	551
22b	Physovenine series (+)-(3a*R*)-2'-methylphenylcarbamate	19.4	11

[*] Estimate Extra Volume = Volume of *R*-Configuration – Enzyme-Excluded Volume Map (Union of Volumes of Active *S*-Configuration Compounds: **9a**, **12a**, **17a** and **22a**).